JAERI-M
83-239

BASIC STUDY OF ELECTRON IRRADIATION TECHNIQUE IN DISINFESTATION PROCESS OF MAIZE

February 1984

Ryuichi TANAKA, Roberto M. URIBE*, Aníbal DE LA PIEDAD* and Esbaide ADEM*

日本原子力研究所
Japan Atomic Energy Research Institute

JAERI-Mレポートは，日本原子力研究所が不定期に公刊している研究報告書です。
入手の問合わせは，日本原子力研究所技術情報部情報資料課（〒319-11茨城県那珂郡東海村）あて，お申しこしください。なお，このほかに財団法人原子力弘済会資料センター（〒319-11 茨城県那珂郡東海村日本原子力研究所内）で複写による実費頒布をおこなっております。

JAERI-M reports are issued irregularly.
Inquiries about availability of the reports should be addressed to Information Section, Division of Technical Information, Japan Atomic Energy Research Institute, Tokai-mura, Naka-gun, Ibaraki-ken 319-11, Japan.

編集兼発行　日本原子力研究所
印　　刷　いばらき印刷㈱

JAERI-M 83-239

BASIC STUDY OF ELECTRON IRRADIATION TECHNIQUE IN DISINFESTATION PROCESS OF MAIZE

Ryuichi TANAKA, Roberto M. URIBE*, Anfbal DE LA PIEDAD*
and Esbaide ADEM*

Department of Development,
Takasaki Radiation Chemistry Research Establishment, JAERI

(Received December 23, 1983)

Electron irradiation technique for disinfestation process of maize is studied on a simple model of continuous-gravity-feed irradiator. Dose and dose rate are evaluated by the calculation of electron current density in the radiation field of a 2.5 MeV electron accelerater assuming the flowing absorber is uniformly distributed.

Various factors contributing to dose dispersion among separate grains are studied in relation to dose uniformity ratio and beam utilization efficiency, and the critical velocity of grains necessary for the dose uniformity after passing through scanned electron beam is obtained.

Dosimetric techniques are also discussed for measurement of absorbed dose and monitoring of irradiation parameters.

Keywords: Electron, Irradiation Technique, Disinfestation, Chemical Radiation Effects, Maiz, Dose, Dose Rate, Dose Dispersion, Dose Uniformity, Beam Utilization Efficiency, Critical Velocity, Dosimetry.

This work was done as a part of a technical cooperative project in Mexico by International Atomic Energy Agency.

* Instituto de Física, Universidad Nacional Autónoma de México, Mexico 20, D.F.

JAERI - M 83 - 239

とうもろこし放射線殺虫プロセスにおける電子線照射技術の基礎研究

日本原子力研究所高崎研究所開発部
田中　隆一・Roberto M. URIBE*・Aníbal DE LA PIEDAD*
Esbaide ADEM*

（1983年12月23日受理）

とうもろこしの放射線殺虫プロセスを開発するため，連続穀粒自由落下方式を用いた電子線照射技術の基礎的検討を行った。吸収線量および線量率の概算は，電子エネルギー 2.5 MeV，吸収体均一分布を仮定し，電子流密度の計算をもとに行った。穀粒間の線量分散に寄与する諸要因を線量均一度および照射利用効率との関連において検討し，線量均一分布を維持するための走査電子ビーム通過時における穀粒の限界速度を求めた。吸収線量の測定および照射パラメータのモニタリングのための技術的手法についても検討した。

本研究は国際原子力機関（IAEA）によるメキシコにおける技術協力プロジェクトの一部として実施された。

＊　国立メキシコ自治大学物理学研究所

CONTENTS

1. Introduction 1
2. A Simple Model of Grain Irradiation 2
3. Calculation of Average Electron Current Density in Irradiation Field 3
4. Calculation of Dose and Dose Rate in Uniformly Distributed Absorber 3
5. Dose Dispersion 5
6. Longitudinal Dose Non-Uniformity with Simultaneuos Absorber Movement and Beam Scanning 7
7. Dose Dispersion in the Depth of Flowing Grains 9
8. Radiation Measurement for the Process 11
9. Other Remarks 13
Acknowledgement 15
References 16
APPENDIX I Calculation of Longitudinal Dose Non-Uniformity with Simultaneous Product Movement and Beam Scanning in Industrial Electron Irradiation 24
APPENDIX II Reference Data on Transmission, Scattering, and Absorption of 2.5 and 3 MeV Electrons in Thick Layer of Matter 36

目　　次

1. 緒　論 …… 1
2. 穀物照射モデル …… 2
3. 照射場における平却電子流密度の計算 …… 3
4. 均一分布吸収体内の線量および線量率の計算 …… 3
5. 線 量 分 散 …… 5
6. 同時的な吸収体移動とビーム走査に伴う縦方向線量不均一性 …… 7
7. 流下穀物深度方向の線量変化 …… 9
8. 放射線測定について …… 11
9. その他の問題点 …… 13
謝　辞 …… 15
参考文献 …… 16
APPENDIX Ⅰ　工業電子線照射における同時的な製品移動とビーム走査に伴う縦方向線量不均一性の計算 …… 24
APPENDIX Ⅱ　厚い物質層に対する2.5 MeVおよび3 MeV電子の透過，散乱および吸収の参考データ …… 36

1. Introduction

Maize is the world's most widely distributed crop and also ranks third in production among major cereal crops, following close behind wheat and rice. About 60% of the world's maize area is found in developing countries. In Latin America, maize is the most important cereal crop, accounting for about 50% of total cereal production. The consumption of maize occupies 73% of total cereal calories in Mexico where about 10^7 tons of maize are cropped per year[1].

However, this amount of maize production is not enough to feed all the population in Mexico and the country has to import more than 10^6 tons of maize every year, because the methods employed in chain production-storage-distribution are very old and rudimentary. There are a great losses in grain due mainly to fungus, rats, birds and insects mainly during the storage time[2]. The FAO considered that the losses in Mexico are between 10 and 25% of the total crop production[3].

Insects cause different kinds of damage to stored grain: the destruction of the grain due to consumption by adults and larvae, contamination by death insects, etc.

In the present, insect control in Mexico is done mainly by the use of pesticides (fumigants and insecticides). In recent years, however, critical situation appeared due to the ecological problem of contamination with the chemical residues, growing costs of chemicals and the development of resistance by some insects.

An alternative to this problem is grain disinfestation by irradiation before storage.

Since 1972 a research program in disinfestation of maize by irradiation has been developed at the Institute of Physics in National Autonomous University of Mexico in order to analyze the possible benefits of this technology[4-7].

Recent activities on this project include the following items:

(1) Determination of disinfestation dosage for common insects in Mexico, using gamma-rays and electron beam.
(2) Preliminary radiation processing studies on the laboratory scale using a 1.5 MeV Van de Graaff electron accelerator.
(3) Chromatological analysis of maize disinfested by irradiation.
(4) Studies on the nutritional quality of irradiated maize.
(5) Studies on the radiation susceptivity of the different insect species.

(6) Comparative study on the effect of humigants and radiation on the nutritional quality of maize.

In basic research on the irradiation effect, gamma-rays have been mainly used, but electron beam will be economically desirable as an industrial process because of the high processing speed and the high utilization efficiency of radiation. The irradiation of grain is more efficient than any other group of foods since grain products can be made to flow through the irradiation field like a fluid. Continuous-flow irradiation systems can be more easily designed for electron radiation processing than for gamma-rays[8].

In application of electron beam as a processing method, for grain disinfestation, however, the irradiation technique becomes a matter of great concern if we want to achieve both requirements of uniform irradiation and high utilization efficiency of radiation. The technique includes more complicated problems in electron irradiation than that in gamma irradiation.

In the present report, we wish to describe the results of the basic study of electron irradiation technique in the disinfestation process of maize.

2. A Simple Model of Grain Irradiation

A simple model of continuous-gravity-feed irradiator for disinfestation of maize with an electron accelerator is illustrated in Fig. 1. Maize grains are transferred through pneumatic feed ducts and irradiated laterally by an horizontally scanned electron beam while they are freely falling vertically down to a container.

The width of grain flow at the exit of the sliding passage of the feed ducts, L_w(cm), is fitted to that of beam scanning of the accelerator. It is assumed that the average flow velocity of the grains v ($cm.s^{-1}$) and the distance from the beam window to the flowing grains are constant during the passage through the irradiation channel in order to simplify the dose calculation.

The increase of the distance results in the decrease of dose rate, but in little decrease of the integrated dose in flowing grains.

The effective thickness of dropping grains is expressed by the equation:

$$t_{ef} = \frac{W_t}{L_w v} \qquad (g.cm^{-2}), \qquad (1)$$

(6) Comparative study on the effect of humigants and radiation on the nutritional quality of maize.

In basic research on the irradiation effect, gamma-rays have been mainly used, but electron beam will be economically desirable as an industrial process because of the high processing speed and the high utilization efficiency of radiation. The irradiation of grain is more efficient than any other group of foods since grain products can be made to flow through the irradiation field like a fluid. Continuous-flow irradiation systems can be more easily designed for electron radiation processing than for gamma-rays[8].

In application of electron beam as a processing method, for grain disinfestation, however, the irradiation technique becomes a matter of great concern if we want to achieve both requirements of uniform irradiation and high utilization efficiency of radiation. The technique includes more complicated problems in electron irradiation than that in gamma irradiation.

In the present report, we wish to describe the results of the basic study of electron irradiation technique in the disinfestation process of maize.

2. A Simple Model of Grain Irradiation

A simple model of continuous-gravity-feed irradiator for disinfestation of maize with an electron accelerator is illustrated in Fig. 1. Maize grains are transferred through pneumatic feed ducts and irradiated laterally by an horizontally scanned electron beam while they are freely falling vertically down to a container.

The width of grain flow at the exit of the sliding passage of the feed ducts, L_w(cm), is fitted to that of beam scanning of the accelerator. It is assumed that the average flow velocity of the grains v ($cm.s^{-1}$) and the distance from the beam window to the flowing grains are constant during the passage through the irradiation channel in order to simplify the dose calculation.

The increase of the distance results in the decrease of dose rate, but in little decrease of the integrated dose in flowing grains.

The effective thickness of dropping grains is expressed by the equation:

$$t_{ef} = \frac{W_t}{L_W v} \qquad (g.cm^{-2}), \qquad (1)$$

where W_t is the flow rate of the grains, that is the throughput. The value of t_{ef} must be taken smaller than the penetration length of incident electrons.

Basic requirements in the irradiation condition which are given for the pilot plant are shown in Table 1.

3. Calculation of Average Electron Current Density in Irradiation Field

Average electron current density distribution for steady current type electron accelerater with single uniform beam scanning in three-dimensional irradiation field can be approximately calculated by a simple formula[9,10] as a function of various irradiation parameters: acceleration voltage, beam current, the material and thickness of beam window, scan geometry, and effective beam diameter.

Fig. 2 shows calculated average electron current density distributions in the direction of maize movement ($j(0,y)$) and in the direction of beam scanning for a typical irradiating condition in the Dynamitron accelerator which is used for the pilot study. Assumed values of irradiation parameters in the calculation are as follows: acceleration voltage is 2.5 MeV, tube current 1 mA, thickness of the beam window 0.06 mm (Ti): total scan width at the beam window 100 cm, scan height 110 cm, the distance from the beam window to maize 20 cm, effective diameter of the electron beam in tube 2 cm (see Appendix I), total mean squared scattering angle 0.039 (see Appendix I), and total transmission coefficient 0.993 (see Appendix I). The peak value of the average electron current density is 0.106 μA cm^{-2}, and the half value width of the electron current density distribution in the direction of maize movement is 7.4 cm.

4. Calculation of Dose and Dose Rate in Uniformly Distributed Absorber

In the irradiation model of Fig. 1, the integrated charge fluence received by the absorber flowing down with a constant velocity v ($cm.s^{-1}$) is given by the equation[9]

$$Q_t = \frac{I_0 \eta_t}{2L'v} \qquad (C.cm^{-2}), \tag{2}$$

where I_0(A) is the beam current in the acceleration tube, N_t the total transmission coefficient, 2L' (cm) the projected scan width on the flowing absorber[9-10].

where W_t is the flow rate of the grains, that is the throughput. The value of t_{ef} must be taken smaller than the penetration length of incident electrons.

Basic requirements in the irradiation condition which are given for the pilot plant are shown in Table 1.

3. Calculation of Average Electron Current Density in Irradiation Field

Average electron current density distribution for steady current type electron accelerater with single uniform beam scanning in three-dimensional irradiation field can be approximately calculated by a simple formula[9,10] as a function of various irradiation parameters: acceleration voltage, beam current, the material and thickness of beam window, scan geometry, and effective beam diameter.

Fig. 2 shows calculated average electron current density distributions in the direction of maize movement ($j(0,y)$) and in the direction of beam scanning for a typical irradiating condition in the Dynamitron accelerator which is used for the pilot study. Assumed values of irradiation parameters in the calculation are as follows: acceleration voltage is 2.5 MeV, tube current 1 mA, thickness of the beam window 0.06 mm (Ti): total scan width at the beam window 100 cm, scan height 110 cm, the distance from the beam window to maize 20 cm, effective diameter of the electron beam in tube 2 cm (see Appendix I), total mean squared scattering angle 0.039 (see Appendix I), and total transmission coefficient 0.993 (see Appendix I). The peak value of the average electron current density is 0.106 μA cm^{-2}, and the half value width of the electron current density distribution in the direction of maize movement is 7.4 cm.

4. Calculation of Dose and Dose Rate in Uniformly Distributed Absorber

In the irradiation model of Fig. 1, the integrated charge fluence received by the absorber flowing down with a constant velocity v ($cm.s^{-1}$) is given by the equation[9]

$$Q_t = \frac{I_0 \eta_t}{2L'v} \qquad (C.cm^{-2}), \tag{2}$$

where I_0(A) is the beam current in the acceleration tube, N_t the total transmission coefficient, 2L' (cm) the projected scan width on the flowing absorber[9-10].

where W_t is the flow rate of the grains, that is the throughput. The value of t_{ef} must be taken smaller than the penetration length of incident electrons.

Basic requirements in the irradiation condition which are given for the pilot plant are shown in Table 1.

3. Calculation of Average Electron Current Density in Irradiation Field

Average electron current density distribution for steady current type electron accelerater with single uniform beam scanning in three-dimensional irradiation field can be approximately calculated by a simple formula[9,10] as a function of various irradiation parameters: acceleration voltage, beam current, the material and thickness of beam window, scan geometry, and effective beam diameter.

Fig. 2 shows calculated average electron current density distributions in the direction of maize movement ($j(0,y)$) and in the direction of beam scanning for a typical irradiating condition in the Dynamitron accelerator which is used for the pilot study. Assumed values of irradiation parameters in the calculation are as follows: acceleration voltage is 2.5 MeV, tube current 1 mA, thickness of the beam window 0.06 mm (Ti): total scan width at the beam window 100 cm, scan height 110 cm, the distance from the beam window to maize 20 cm, effective diameter of the electron beam in tube 2 cm (see Appendix I), total mean squared scattering angle 0.039 (see Appendix I), and total transmission coefficient 0.993 (see Appendix I). The peak value of the average electron current density is 0.106 μA cm^{-2}, and the half value width of the electron current density distribution in the direction of maize movement is 7.4 cm.

4. Calculation of Dose and Dose Rate in Uniformly Distributed Absorber

In the irradiation model of Fig. 1, the integrated charge fluence received by the absorber flowing down with a constant velocity v ($cm.s^{-1}$) is given by the equation[9]

$$Q_t = \frac{I_0 \eta_t}{2L'v} \qquad (C.cm^{-2}), \tag{2}$$

where I_0(A) is the beam current in the acceleration tube, N_t the total transmission coefficient, 2L' (cm) the projected scan width on the flowing absorber[9-10].

Assuming that the flowing absorber is uniformly distributed within a fixed thickness which nearly equals the extrapolation range of incident electrons, the depth dose distribution in the absorber after passing through the electron beam is approximately expressed by the equation:

$$D(z) = 5 \times 10^8 \frac{I_0 \eta_t}{L'v} I(z) \qquad (Gy), \tag{3}$$

where $I(z)$ ($MeV \cdot cm^2 \cdot g^{-1}$) is energy deposited per unit thickness ($g \cdot cm^{-2}$) at the depth z, assuming that one electron$\cdot cm^{-2}$ is generated at source plane[11].

Figure 3 shows the distribution of $I(z)$ in a water medium for plane perpendicular beam of 2.5 MeV monoenergetic electrons given by Tabata's empirical formula[12]. The value of $I(0)$ is almost the same as that of mass collision stopping power for water at 2.5 MeV, but is little smaller than that value. The difference is mainly due to the effect of delta-ray production. The calculated profile of $I(z)$ can be approximately applied for the depth dose profile in the flowing water absorber exposed by electrons which have 2.5 MeV before passing through the beam window, since the electron energy loss and the scattering in the beam window and air are usually not enough large to cause significant change in the profile.

The average dose rate at an arbitrary point in the absorber passing through the radiation field changes with time t (s) as follows:

$$\dot{D}(t) = \frac{5 \times 10^8 I_0 \eta_t I(z)}{RL'\sqrt{\pi\, \bar{\theta}_t^2}} \exp\left(- \frac{v^2 (t-t_0)^2}{R^2 \bar{\theta}_t^2} \right) \quad (Gy \cdot s^{-1}), \tag{4}$$

where t_0 is the time when the point in the absorber crosses the fan-shaped plane ($y = 0$) formed by beam scanning and R (cm) the distance from the beam window to the flowing grains, $\bar{\theta}_t^2$ the total mean squared scattering angle.

From equation (4), the peak value of the average dose rate by the equation can be obtained as

$$\dot{D}_p = \frac{5 \times 10^8 I_0 \eta_t I(z)}{RL'\sqrt{\pi\, \bar{\theta}_t^2}} \qquad (Gy \cdot s^{-1}). \tag{5}$$

The absorbed dose rate according to eq. (4) is the value obtained by averaging the periodic change due to beam scanning[9-10]. The peak

value of the real dose rate is usually much higher than $\dot{D}_p$. The ratio of the real value of the real dose rate to $\dot{D}_p$ under the assumption $R\sqrt{\overline{\theta_t^2}} \ll L'$ is given by the equation:

$$r = \frac{2L'}{R\sqrt{\pi\ \overline{\theta_t^2}}} . \qquad (6)$$

The value of the ratio is about 16 in the assumed irradiation condition described above.

5. Dose Dispersion

The radiation process should be conducted so as the satisfy that a minimum value of the dose in the absorber D_{min} is greater than or equal to the lowest permissible dose D_{lp}, and that a maximum value of the dose D_{max} is lower than or equal to the highest permissible dose D_{hp}. Even if the highest permissible dose is not definite, the maximum value must be minimized for economical and nutritional reasons. These considerations usually result in a choice of a low value of the dose uniformity ratio, D_{max}/D_{min}.

When the absorber is a bulk material, the values of D_{min} and D_{max} are usually given at the definite position in the absorber depending on the shape of the absorber, the irradiation sources and the irradiation methods. When the absorber consists of flowing grains, however, the spacial dose distribution cannot be defined but the values of D_{min} and D_{max} may be treated as two extreme values in statistical dose variation in the irradiated grains.

The statistical dose variation in grains can be divided into the dose variation in each grain and the dose dispersion among grains.

The former depends on the average grain size and shape. It will be negligibly small, if the dimension of the grain is much smaller than the penetration length of the incident electrons. The average dimension of the grains in various kinds of maizes is roughly in the same order of the range of a few MeV electrons, so that the dose distribution in the grain cannot be neglected.

The statistical fluctuation of the dose variation also depends on the average dimension of the flowing grains, the flowing condition such as the rotation of the grains, the backscattering materials behind the flow, etc. The rotation of the grain has a tendency to make the dose distribution uniform, and the rotation angle within the time interval

value of the real dose rate is usually much higher than $\dot{D}_p$. The ratio of the real value of the real dose rate to $\dot{D}_p$ under the assumption $R\sqrt{\overline{\theta_t^2}} \ll L'$ is given by the equation:

$$r = \frac{2L'}{R\sqrt{\pi\ \overline{\theta_t^2}}} . \qquad (6)$$

The value of the ratio is about 16 in the assumed irradiation condition described above.

5. Dose Dispersion

The radiation process should be conducted so as the satisfy that a minimum value of the dose in the absorber D_{min} is greater than or equal to the lowest permissible dose D_{lp}, and that a maximum value of the dose D_{max} is lower than or equal to the highest permissible dose D_{hp}. Even if the highest permissible dose is not definite, the maximum value must be minimized for economical and nutritional reasons. These considerations usually result in a choice of a low value of the dose uniformity ratio, D_{max}/D_{min}.

When the absorber is a bulk material, the values of D_{min} and D_{max} are usually given at the definite position in the absorber depending on the shape of the absorber, the irradiation sources and the irradiation methods. When the absorber consists of flowing grains, however, the spacial dose distribution cannot be defined but the values of D_{min} and D_{max} may be treated as two extreme values in statistical dose variation in the irradiated grains.

The statistical dose variation in grains can be divided into the dose variation in each grain and the dose dispersion among grains.

The former depends on the average grain size and shape. It will be negligibly small, if the dimension of the grain is much smaller than the penetration length of the incident electrons. The average dimension of the grains in various kinds of maizes is roughly in the same order of the range of a few MeV electrons, so that the dose distribution in the grain cannot be neglected.

The statistical fluctuation of the dose variation also depends on the average dimension of the flowing grains, the flowing condition such as the rotation of the grains, the backscattering materials behind the flow, etc. The rotation of the grain has a tendency to make the dose distribution uniform, and the rotation angle within the time interval

when the grain pass through the electron beam depends on the flow velocity and the effective width of the electron beam which is proportional to $R\sqrt{\overline{\theta_t^2}}$.

The statistical dose variation means the dispersion of the average dose in each irradiated grain among a number of grains. The dose dispersion is supposed to be significant and complicated especially in electron irradiation of grains of maize. The factors influencing the dose dispersion can be classified roughly in following four groups.

The first group is the change of the integrated charge fluence Q_t with time. The factors contributing to the changes of Q_t are as follows:

(1) Instability of the flow velocity of maize.

(2) Fluctuation of the beam current.

(3) The fluctuation of the scan width followed by that of the acceleration voltage.

The factor (1) is regarded as the most important of the three factors in the actual process.

The second group is the lateral variation of the depth dose distribution D(z). The factors contributing to the variations are as follows:

(1) Longitudinal dose non-uniformity with simultaneous grains movement and beam scanning (see Appendix I) (in the direction of the motion of maize).

(2) Transversal dose non-uniformity due to the non-uniformity of scanned beam intensity and the scanning geometry.

(3) Transversal non-uniformity of the flow velocity (in the scanning direction).

The factor (1) means the dose non-uniformity due to imperfection of multiple overlap of successive scan traces. This overlap is basically necessary to avoid the dose non-uniformity in electron radiation processing. The requirement is a critical problem in the field of food irradiation processing using powerful electron accelerators in which the required doses are 1 kGy or lower and consequently the velocity of products are very high. A theoretical estimation of the requirements is described later.

The factor (2) depends on the deflection angle of scanned electrons and the distance from the beam window to the flowing grains R. It can be improved by a suitable choice of the wave form of electric current through the scanning magnet.

The third group is the dose variation in the depth of flowing grains. The factors contributing to the variation are as follows:

(1) The effective thickness of the flowing grains,
(2) The fluctuation of the effective thickness of the flowing grains,
(3) The flowing condition such as the rotation of grains,
(4) The variation of I(z) due to the fluctuation of acceleration voltage.

The factor (1) is closely connected with other three factors. The factor (2) can be divided into two different variations. One is the change with time of the effective thickness or flow rate of grains. The other is the spacial probability distribution of the effective thickness due to uneven distribution of grains. The latter is basically important in consideration of the dose dispersion in flowing grains due to electron irradiation.

The fourth group is associated with the statistical fluctuations found in the irradiation plant, which belongs to different kinds of factors from the three groups described above. The factors contributing to the fourth group are as follows:

(1) Uncertainties in measuring average doses in grains,
(2) Fluctuation in plant operation parameter settings,
(3) Uncertainties in measuring the plant operation parameters.

The factors (2) and (3) result in fluctuations in the dose values in grains. The dosimetrical problem in grain irradiation process is described in a later section.

Of all the factors influencing the dose dispersion, several factors can be theoretically or experimentally estimated. However, it is not easy to quantitatively treat a few factors in relation to the flowing condition and the fluctuation of the effective absorber thickness.

The overall dose dispersion which can be obtained by measuring the dose variation in irradiated grains includes all the contributions of these factors. Therefore, the result of the dose measurements obtained by a random sampling method may give some useful information about these uncertain factors.

In this report, we considered some basic parameters of all those described above quantitatively or qualitatively.

6. Longitudinal Dose Non-uniformity with Simultaneous Absorber Movement and Beam Scanning

In Appendix 1, we give the fundamental formula generalizing the

The third group is the dose variation in the depth of flowing grains. The factors contributing to the variation are as follows:

(1) The effective thickness of the flowing grains,
(2) The fluctuation of the effective thickness of the flowing grains,
(3) The flowing condition such as the rotation of grains,
(4) The variation of I(z) due to the fluctuation of acceleration voltage.

The factor (1) is closely connected with other three factors. The factor (2) can be divided into two different variations. One is the change with time of the effective thickness or flow rate of grains. The other is the spacial probability distribution of the effective thickness due to uneven distribution of grains. The latter is basically important in consideration of the dose dispersion in flowing grains due to electron irradiation.

The fourth group is associated with the statistical fluctuations found in the irradiation plant, which belongs to different kinds of factors from the three groups described above. The factors contributing to the fourth group are as follows:

(1) Uncertainties in measuring average doses in grains,
(2) Fluctuation in plant operation parameter settings,
(3) Uncertainties in measuring the plant operation parameters.

The factors (2) and (3) result in fluctuations in the dose values in grains. The dosimetrical problem in grain irradiation process is described in a later section.

Of all the factors influencing the dose dispersion, several factors can be theoretically or experimentally estimated. However, it is not easy to quantitatively treat a few factors in relation to the flowing condition and the fluctuation of the effective absorber thickness.

The overall dose dispersion which can be obtained by measuring the dose variation in irradiated grains includes all the contributions of these factors. Therefore, the result of the dose measurements obtained by a random sampling method may give some useful information about these uncertain factors.

In this report, we considered some basic parameters of all those described above quantitatively or qualitatively.

6. Longitudinal Dose Non-uniformity with Simultaneous Absorber Movement and Beam Scanning

In Appendix 1, we give the fundamental formula generalizing the

relation between the dose non-uniformity and irradiation parameters for steady current type electron accelerators with single beam scanning. From this consideration we obtained the critical velocity of the absorber necessary for the longitudinal dose uniformity as follows:

$$v_c = fR\sqrt{\overline{\theta_t^2}} \quad , \tag{7}$$

where f is the scan frequency (Hz). In the case of the Dynamitron eq. (7) is expressed in the form, $v_c \simeq 50\ R\ (cm \cdot s^{-1})$ since f = 100 Hz and $\sqrt{\overline{\theta_t^2}} \simeq 0.04$ for the acceleration voltage of 2.5 MeV.

If we consider the effective diameter of the electron beam in the accelerator tube δ (cm), eq. (7) is more correctly expressed in the form, $v_c = 100\sqrt{0.04R^2 + \delta^2/4}\ (cm \cdot s^{-1})$. When R = 10 cm and δ = 4 cm, the critical velocity equals 2.8 $m \cdot s^{-1}$.

The critical beam current in the acceleration tube necessary for the longitudinal dose uniformity is given by the equation (see Appendix 1)

$$I_c = \frac{2 \times 10^{-9} v_c L' D_{max}}{\eta_t I(z)_{max}} \quad (A), \tag{8}$$

where D_{max} (Gy) is the maximum dose which is required for the disinfestation, L' a half of the projected scan width on the flowing grains, $I(z)_{max}$ the maximum value of $I(z)(MeV \cdot cm^2\ g^{-1})$, the energy deposited per unit thickness $(g.cm^{-2})$ at the depth z, assuming that one electron cm^{-2} is generated at source plane, and η_t is the total transmission coefficient. Assuming that the required maximum dose is 1 kGy for disinfestation of maize, L' = 55 cm, $I(z)_{max}$ = 2.7 and η_t = 1, the critical current equals 17.4 mA.

The critical value of the throughput, i.e. the amount of product to be treated with a given dose within a defined period of time, is given by the equation (see Appendix I)

$$W_t = \frac{2 \times 10^{-9} f_e v_c L' E_0 D_{max}}{\eta_t I(z)_{max} \bar{D}} \tag{9}$$

where f_e is the utilization efficiency of electron energy, $\bar{D}$ the average absorbed dose in the maize. Assuming that f_e = 0.5 and $\bar{D}$ = 0.4 kGy, the critical value of the throughput equals 128 $ton \cdot h^{-1}$.

If the maximum dose in the flowing grains can be reduced to a smaller value than the required maximum dose (the highest permissible

dose), D_{hp}, the effective critical beam current will decrease. In the case of the disinfestation process of maize, the maximum dose in the grains can be reduced to much smaller value than the value of D_{hp} (1 krad), since the required minimum value D_{lp} is 70 Gy. If the dose uniformity ratio is 2, the maximum dose in the grains is 140 Gy, and this value results in a small critical current for the longitudinal dose non-uniformity ($\simeq$ 1.6 mA), and a critical value of the throughput ($\simeq$ 18 ton·h^{-1}) for the previous assumption.

Since the utilization efficiency is estimated to the smaller than 0.5 for grain irradiation processes, the calculated results suggests that it is necessary to increase the scan frequency and/or the distance from the beam window to flowing grains for longitudinal dose uniformity, if the required throughput for the irradiation plant is more than 100 ton·h^{-1}.

7. Dose Variation in the Depth of Flowing Grains

The most important feature of electron beam irradiation is that the penetration length is short and it results in large dose variation within the penetration length. The existance of a build-up of dose in plane perpendicular beam irradiation complicates the positioning of depths giving the maximum dose D_{max} and the minimum dose D_{min}. The positioning is more complicated by the influence of backscattering from materials behind the absorber.

In a rough idea in which the influence of backscattering is simplified, dose dispersion with increase of the absorber thickness t_a can be classified into three regions as shown in Fig. 4: (A) $0 < t_a \leq z_p$, (B) $z_p < t_a \leq z_{ef}$ and (C) $z_{ef} < t_a \leq z_{max}$, where z_p is the depth giving the peak dose and z_{ef} is the depth giving the same dose as the surface dose. The value of D'_{min} equals the surface dose in (A) and (B) and that of D'_{max} equals the peak dose in (B) and (C).

Figure 5 shows the change of uniformity ratio D'_{max}/D'_{min} and utilization efficiency in the depth dose curve with the absorber thickness. The increase of the thickness raises the utilization efficiency but lowers the uniformity.

In the irradiation of continuously flowing grains, the effective thickness of the absorber is not constant, for the reason that there is the fluctuation of average effective thickness of lowing grains and the

dose), D_{hp}, the effective critical beam current will decrease. In the case of the disinfestation process of maize, the maximum dose in the grains can be reduced to much smaller value than the value of D_{hp} (1 krad), since the required minimum value D_{lp} is 70 Gy. If the dose uniformity ratio is 2, the maximum dose in the grains is 140 Gy, and this value results in a small critical current for the longitudinal dose non-uniformity ($\simeq$ 1.6 mA), and a critical value of the throughput ($\simeq$ 18 ton·h^{-1}) for the previous assumption.

Since the utilization efficiency is estimated to the smaller than 0.5 for grain irradiation processes, the calculated results suggests that it is necessary to increase the scan frequency and/or the distance from the beam window to flowing grains for longitudinal dose uniformity, if the required throughput for the irradiation plant is more than 100 ton·h^{-1}.

7. Dose Variation in the Depth of Flowing Grains

The most important feature of electron beam irradiation is that the penetration length is short and it results in large dose variation within the penetration length. The existance of a build-up of dose in plane perpendicular beam irradiation complicates the positioning of depths giving the maximum dose D_{max} and the minimum dose D_{min}. The positioning is more complicated by the influence of backscattering from materials behind the absorber.

In a rough idea in which the influence of backscattering is simplified, dose dispersion with increase of the absorber thickness t_a can be classified into three regions as shown in Fig. 4: (A) $0 < t_a \leq z_p$, (B) $z_p < t_a \leq z_{ef}$ and (C) $z_{ef} < t_a \leq z_{max}$, where z_p is the depth giving the peak dose and z_{ef} is the depth giving the same dose as the surface dose. The value of D'_{min} equals the surface dose in (A) and (B) and that of D'_{max} equals the peak dose in (B) and (C).

Figure 5 shows the change of uniformity ratio D'_{max}/D'_{min} and utilization efficiency in the depth dose curve with the absorber thickness. The increase of the thickness raises the utilization efficiency but lowers the uniformity.

In the irradiation of continuously flowing grains, the effective thickness of the absorber is not constant, for the reason that there is the fluctuation of average effective thickness of lowing grains and the

spacial probability distribution of the effective thickness due to uneven distribution of grains. This results in increase of dose variation among the irradiated grains. The contribution to the dose variation probably is larger in the latter fluctuation than in the former one. The width and the shape of the spacial probability distribution depends on the size and shape of the grain, the flowing rate and also probably on the flowing condition.

Figure 6 shows typical examples of the relative frequency distributions of average doses in separate irradiated grains for given relative probability distributions in three different regions of the effective thickness. When the maximum value of the effective thickness t_{max} is less than z_{ef} ((a) in Fig. 6), the dose variation is limited within a narrow region as shown in (A) and (B) in Fig. 4. The utilization efficiency in these conditions strongly depends on the width and the shape of the probability distribution.

When $z_{ef} < t_{max} \leq z_{max}$, ((b) in Fig. 6), the frequency distribution has a long tail on the lower dose side of the distribution and the value of D'_{min} critically determines not only the uniformity ratio but also the effectiveness of disinfestation. The value of D'_{min} must be more than the lowest permissible dose for disinfestation, D_{lp}, but it is not easy to control the value of D'_{min}, since D'_{min} changes quite sensitively with t_{max} in this region of the depth. The beam utilization efficiency in this condition does not strongly depend on the probability distribution itself.

When $z_{max} \leq t_{max}$ ((c) in Fig. 6), the irradiation becomes clearly ineffective for disinfestation, even if the average value of the effective thickness is less than z_{ef}.

In the three cases described above, the values of D'_{max} always equal the peak of the depth dose curve (broken lines in Fig. 4). Even if we consider unevenly distribution of grains, D'_{max} is considered to be almost determined by Q_t in eq. (2) and does not almost depend on the effective thickness. Therefore, D'_{min} is a decisive factor for dose uniformity ratio, if we neglect the fluctuations of other irradiation parameters.

If the values of t_{max} is less than z_{max}, the depth dose distribution is influenced by electron backscattering from the material behind the flowing absorber. Figure 7 shows typical examples of the depth dose curves in thin absorbers compared with the maximum electron range z_{max}.

If there is no scattering material behind the absorber, the dose value is less than that in the full depth dose curve as shown in Fig. 7 (a). The dose difference is large near the back side of the absorber, and the range of the depth suffering the apparent dose reduction depends on the thickness of the absorber. The dose reduction near the back side lowers the uniformity ratio in the thickness region of (B) and (C) in Fig. 5, so that some scattering material is necessary for improvement of the dose uniformity.

If there is any scattering material with higher effective atomic number behind the absorber, the dose value is more than that in the full depth dose curve as shown in Fig. 7 (b). The dose difference is large near the back side of the absorber and also large for the scattering material with high atomic number. The backscattering contributes not only to improvement of the utilization efficiency of electron energy, but also the improvement of the uniformity ratio in (B) and (C) region in Fig. 5 as shown in Fig. 7 (a). In the thickness region of (A), however, the uniformity ratio is reduced by backscattering as shown in Fig. 7 (b).

Figure 8 shows the distribution of I(z) in a water medium for plane perpendicular beam of different monoenergetic electrons. The basic profile is similar in higher energies than 2.5 MeV, but the ratio of the effective range z_{ef} to the incident electron energy increases a little with electron energy, and also the ratio of the surface to maximum dose decreases with electron energy. These characteristics show that the utilization efficiency and the uniformity ratio is improved with increase of electron energy to some extent. These factors are also estimated to be improved with increase of electron energy in consideration of spacial probability distribution of the effective thickness due to uneven distribution of grains.

8. Radiation Measurement for the Process

Radiation dosimetry plays two important roles in radiation processing for disinfestation of maize: One is measurement of absorbed dose in irradiated grains, and another is dosimetrical monitoring of some irradiation parameters. The first one includes the measurement of the dose dispersion among grains and that of dose variation in each grain.

In the measurement of the dose dispersion, it is necessary to

If there is no scattering material behind the absorber, the dose value is less than that in the full depth dose curve as shown in Fig. 7 (a). The dose difference is large near the back side of the absorber, and the range of the depth suffering the apparent dose reduction depends on the thickness of the absorber. The dose reduction near the back side lowers the uniformity ratio in the thickness region of (B) and (C) in Fig. 5, so that some scattering material is necessary for improvement of the dose uniformity.

If there is any scattering material with higher effective atomic number behind the absorber, the dose value is more than that in the full depth dose curve as shown in Fig. 7 (b). The dose difference is large near the back side of the absorber and also large for the scattering material with high atomic number. The backscattering contributes not only to improvement of the utilization efficiency of electron energy, but also the improvement of the uniformity ratio in (B) and (C) region in Fig. 5 as shown in Fig. 7 (a). In the thickness region of (A), however, the uniformity ratio is reduced by backscattering as shown in Fig. 7 (b).

Figure 8 shows the distribution of I(z) in a water medium for plane perpendicular beam of different monoenergetic electrons. The basic profile is similar in higher energies than 2.5 MeV, but the ratio of the effective range z_{ef} to the incident electron energy increases a little with electron energy, and also the ratio of the surface to maximum dose decreases with electron energy. These characteristics show that the utilization efficiency and the uniformity ratio is improved with increase of electron energy to some extent. These factors are also estimated to be improved with increase of electron energy in consideration of spacial probability distribution of the effective thickness due to uneven distribution of grains.

8. Radiation Measurement for the Process

Radiation dosimetry plays two important roles in radiation processing for disinfestation of maize: One is measurement of absorbed dose in irradiated grains, and another is dosimetrical monitoring of some irradiation parameters. The first one includes the measurement of the dose dispersion among grains and that of dose variation in each grain.

In the measurement of the dose dispersion, it is necessary to

evaluate the average dose in each grain by distributing a certain number of dosemeter pieces into the grains. There are the following main dosimetric requirement for this purpose:

(1) The dosimeter piece including its capsule is equivalent to the grain of maize in the size, the shape, the density and the behaviour.

(2) The available dose range of the dose meter is from tens to hundreds of Gy.

(3) The dose meter material is approximately equivalent to maize in the effective atomic number.

(4) The precision of the dose meter is good (< 5%) in consideration of estimation of the influences of irradiation parameters on the dose dispersion.

(5) The handling and read-out procedures of the dose meter are simple.

The last requirement is important, since a number of dose meter pieces are necessary to obtain a dose dispersion curve.

The practical dose meters which may satisfy these requirements at the present are as follows:

(1) Thermoluminescence dose meter (TLD)[13].

(2) Lyoluminescence dose meter[14,15].

(3) Alanine dose meter[16].

TLD is the most convenient system for the required dose range but most phosphers do not have very good precision or reproducibility in the high dose range. The alanine dose meter, a free radical dose meter using electron spin resonance (ESR), is the most precise method of all the solid state dosimetry systems for high dose region, and also the equivalence to organic materials is quite good. However, it is not so practical now for the reason that it requires a well controlled ESR machine and some other special techniques to maintain the good reproducibility. Lyoluminescence dose meter has also good equivalence to organic materials, but is not still practical compared with TLD.

The dose variation in a grain of maize is not much important compared with the dose dispersion among grains, but the dose variation in a grain is relatively larger in electron irradiation than gamma and X-ray irradiation. Special microphoto-densitometric technique using thin plastic or dyed plastic dose meters is necessary for the measurement of the dose distribution.

Some radiochromic dye dosimeters[17,18] and CTA dose meter are

suitable for this purpose[19,20]. A small dose meter strip is inserted into a section of the grain, and after irradiation, the optical density distribution in the strip can be measured with a microspectrophotometer. If the dose variation in a grain is large compared with the dose dispersion among grains, it may be necessary to change the condition of the grain flow or to increase the electron energy.

Another application of dosimetric systems to this disinfestation process is monitoring of irradiation parameters such as the flow rate of grains.

The real time monitoring of the flow rate can be done by the detector head of dose rate meters to measure bremsstrahlung X-ray from the scattering plate of high atomic number behind the flowing grains. The change in the effective thickness of flowing grains results in that of the intensity of X-rays. The responce of the dose rate meter is given by a function of the thickness depending on the geometrical arrangement. If the flow velocity is constant, the responce is also a function of the flow rate. Silicon solar cell dose rate meter which has radiation resistance may be suitable for the monitoring device[21,22]. The monitoring of the flow rate in the direction of beam scanning can be carried out by placing the detector heads at regular intervals along the scan direction.

The average thickness of the flowing grains for a certain period of irradiation may be monitored by some integrating dose meter for very large dose region which is placed just behind the flowing grains. The relationship between the thickness and the measured dose, however, may be not simplified by electron backscattering from the scattering plate.

9. Other Remarks

The most important parameter to control is the dose dispersion among the grains for irradiation technique in electron radiation process of maize. It is quite easy to satisfy the basic requirement that the dose uniformity ratio must be smaller than the value of D_{hp}/D_{lp} ($\simeq 14$), but the maximum dose must be reduced as much as possible for economical reasons and to minimize some kind of radiation damage in food. Therefore, we have to consider the three following basic requirements for this process from the point of view of irradiation technique: (1) the minimum dose in the absorber must be greater than the lowest permissible dose, 70 Gy, (2) the dose uniformity ratio must be reduced as much as possible,

suitable for this purpose[19,20]. A small dose meter strip is inserted into a section of the grain, and after irradiation, the optical density distribution in the strip can be measured with a microspectrophotometer. If the dose variation in a grain is large compared with the dose dispersion among grains, it may be necessary to change the condition of the grain flow or to increase the electron energy.

Another application of dosimetric systems to this disinfestation process is monitoring of irradiation parameters such as the flow rate of grains.

The real time monitoring of the flow rate can be done by the detector head of dose rate meters to measure bremsstrahlung X-ray from the scattering plate of high atomic number behind the flowing grains. The change in the effective thickness of flowing grains results in that of the intensity of X-rays. The responce of the dose rate meter is given by a function of the thickness depending on the geometrical arrangement. If the flow velocity is constant, the responce is also a function of the flow rate. Silicon solar cell dose rate meter which has radiation resistance may be suitable for the monitoring device[21,22]. The monitoring of the flow rate in the direction of beam scanning can be carried out by placing the detector heads at regular intervals along the scan direction.

The average thickness of the flowing grains for a certain period of irradiation may be monitored by some integrating dose meter for very large dose region which is placed just behind the flowing grains. The relationship between the thickness and the measured dose, however, may be not simplified by electron backscattering from the scattering plate.

9. Other Remarks

The most important parameter to control is the dose dispersion among the grains for irradiation technique in electron radiation process of maize. It is quite easy to satisfy the basic requirement that the dose uniformity ratio must be smaller than the value of D_{hp}/D_{lp} ($\simeq 14$), but the maximum dose must be reduced as much as possible for economical reasons and to minimize some kind of radiation damage in food. Therefore, we have to consider the three following basic requirements for this process from the point of view of irradiation technique: (1) the minimum dose in the absorber must be greater than the lowest permissible dose, 70 Gy, (2) the dose uniformity ratio must be reduced as much as possible,

(3) the beam utilization efficiency must be raized as much as possible.

In higher beam utilization efficiency, however, the value of D_{min} changes very sensitively with the maximum value of the effective thickness and the dose uniformity is poor as shown in Fig. 6. This means that the first and second requirements are incompatible with the third one. Some optimization will be necessary in consideration of the priority order of the requirement.

When we refer to the effective beam utilization efficiency, there are four kinds of beam power loss contributing to the efficiency as follows:

(1) Escape of energy in the forms of electron penetration through the absorber and electron backscattering from the absorber.

(2) Waste of energy in the form of excess dose in the absorber over the effective dose where the beneficial effect of radiation can saturate.

(3) Escape of energy due to over-scanning of the electron beam on both sides of the flowing absorber, which cannot be avoided to guarantee a sufficiently uniform dose across the width of the absorber.

(4) Dissipation of energy in the beam window of the accelerator and in the air layer.

In the first and third contributions, some part of the escaping energy can be reused by electron scattering from some scattering material with high atomic number. The third and fourth contributions can be easily estimated for the Dynamitron accelerator. They may not exceed 10 or 15% of the total beam energy for the wide scan width (2L) above 100 cm. The amount of the first and second contributions depend on the average effective thickness of the flowing grains and the probability distribution in the effective thickness, so that they cannot be accurately estimated by theoretical calculation. It is assumed that the net amounts exceeds 50% of the total incident energy even for the optimum irradiation condition for the disinfestation process.

In the calculations of dose and dose uniformity, the flow velocity of grains is assumed to be constant in this report. In the model of the continuous-gravity-feed irradiator, however, the real flow velocity increases in the radiation field by the acceleration of gravity. If the mean valocity, which may be given as the velocity when the grains cross the fan-shaped plane ($y = 0$) formed by beam scanning, is used in the calculation, the influence of the acceleration on the calculated results

is not considered to be significant in typical irradiation conditions. However, if the mean velocity is very low or the distance from the beam window to the flowing grain, R, is very long, the influence will not be neglected, since the flow velocity suffers significant change in the radiation field.

Another influence of the acceleration of gravity is the change of the effective thickness of the flowing grains along the flow line. The increase of the velocity results in the decrease of the effective thickness, since the flow rate of the grain is constant along the flow line. This problem may not be neglected in consideration of dose uniformity and beam utilization efficiency.

The dose uniformity is lower at the entrance of the radiation field than at the exit. This influence is also important when the mean velocity is relatively low or R is relatively long.

Acknowledgement

The Authers are grateful to Mr. S. Tanaka and Mr. T. Kanazawa for their helps in the calculation using ETRAN code for Appendix II.

is not considered to be significant in typical irradiation conditions. However, if the mean velocity is very low or the distance from the beam window to the flowing grain, R, is very long, the influence will not be neglected, since the flow velocity suffers significant change in the radiation field.

Another influence of the acceleration of gravity is the change of the effective thickness of the flowing grains along the flow line. The increase of the velocity results in the decrease of the effective thickness, since the flow rate of the grain is constant along the flow line. This problem may not be neglected in consideration of dose uniformity and beam utilization efficiency.

The dose uniformity is lower at the entrance of the radiation field than at the exit. This influence is also important when the mean velocity is relatively low or R is relatively long.

Acknowledgement

The Authers are grateful to Mr. S. Tanaka and Mr. T. Kanazawa for their helps in the calculation using ETRAN code for Appendix II.

References

(1) CIMMIT Report One, "World Maiz Facts and Trends", Interm. Maiz and Wheat Improvement Center, México.

(2) Steering Committee for Study on Postharvest Food Losses in Developing Countries, "Postharvest Food Losses in Developing Countries", National Academy of Sciences, Washington, D.C. (1978).

(3) Gree, A.E., "An Analysis of an FAO Survey of Post Harvest Food Losses in Developing Countries", AGP Document AGPP: MISC/27, FAO Rome, March (1979).

(4) Adem, E., Uribe, R.M., Anibal de la Piedad, and Reyes, L.J., Radiat Phys. Chem. 9, 763 (1977).

(5) Adem, E., Uribe, R.M., and Watters, F.L., Radiat. Phys. Chem. 14, 663 (1979).

(6) Adem, R., Uribe, R.M., Watters, F.L., and Bourges, H., Radiat Phys. Chem. 18, 555 (1981).

(7) Uribe, R.M., "Food Irradiation in México", 3rd IFFIT Inter-Regional Training Cource on Food Irradiation, Wageningen, Holland, IAEA (1981).

(8) STI/DOC/10/178, "Manual of Food Irradiation Dosimetry", IAEA, Vienna (1977).

(9) Tanaka, R., Oyo Butsuri 48, 432 (1979) (in Japanese).

(10) Tanaka, R., Sunaga, H., Yotsumoto, K., Mizuhashi, K., and Tamura, N., Radiation Phys. Chem. 18, 927 (1981).

(11) Spencer, L.V., NBS Monograph 1, National Bureau of Standards (1959).

(12) Tabata, T., and Ito, R., Nucl. Sci. Eng. 53, 226 (1974).

(13) Uribe, R.M., and Puente, R., Radiat. Phys. Chem. 13, 191 (1979).

(14) Regulla, D.F., and Deffner, U., Int. J. Appl. Radiat. Isot. 33, 1101 (1982).

(15) Ettinger, K.V., and Puite, K.J., Intern. J. Appl. Radiat. Isot. 33, 1115 (1982).

(16) Puite, K.J., and Ettinger, K.V., Intern. J. Appl. Radiat. Isot. 33, 1139 (1982).

(17) McLaughlin, W.L., In Manual on Radiation Dosimetry (Edited by Horm, N.W. and Berry, J.R.), p. 378, Marcel Dekker, New York (1970).

(18) Kantz, A.D., and Humpherys, C., Radiat. Phys. Chem. 18, 937 (1981).

(19) Tamura, N., Tanaka, R., Mitomo, S., Matsuda, K., and Nagai, S., Radiat. Phys. Chem. 18, 947 (1981).

(20) Tanaka, R., Mitomo, S., and Tamura, N., Intern. J. Appl. Radiat. Isot., In press.

(21) Tanaka, R., Tajima, T., and Usami, A., Inter. J. Appl. Radiat. Isot. 24, 627 (1973).

(22) Tanaka, R., Tajima, T., and Usami, A., Intern. J. Appl. Radiat. Isot. 27, 73 (1976).

Table 1 Basic requirements in the irradiation condition which are given for the pilot plant of disinfestation process of maize.

Highest permissible dose,	D_{hp}:	1000 Gy
Lowest permissible dose,	$D_{\ell p}$:	70 Gy
Electron energy,	E_o	2.5 MeV
Throughput,	W_t	: 7 ∿ 10 ton $\cdot h^{-1}$

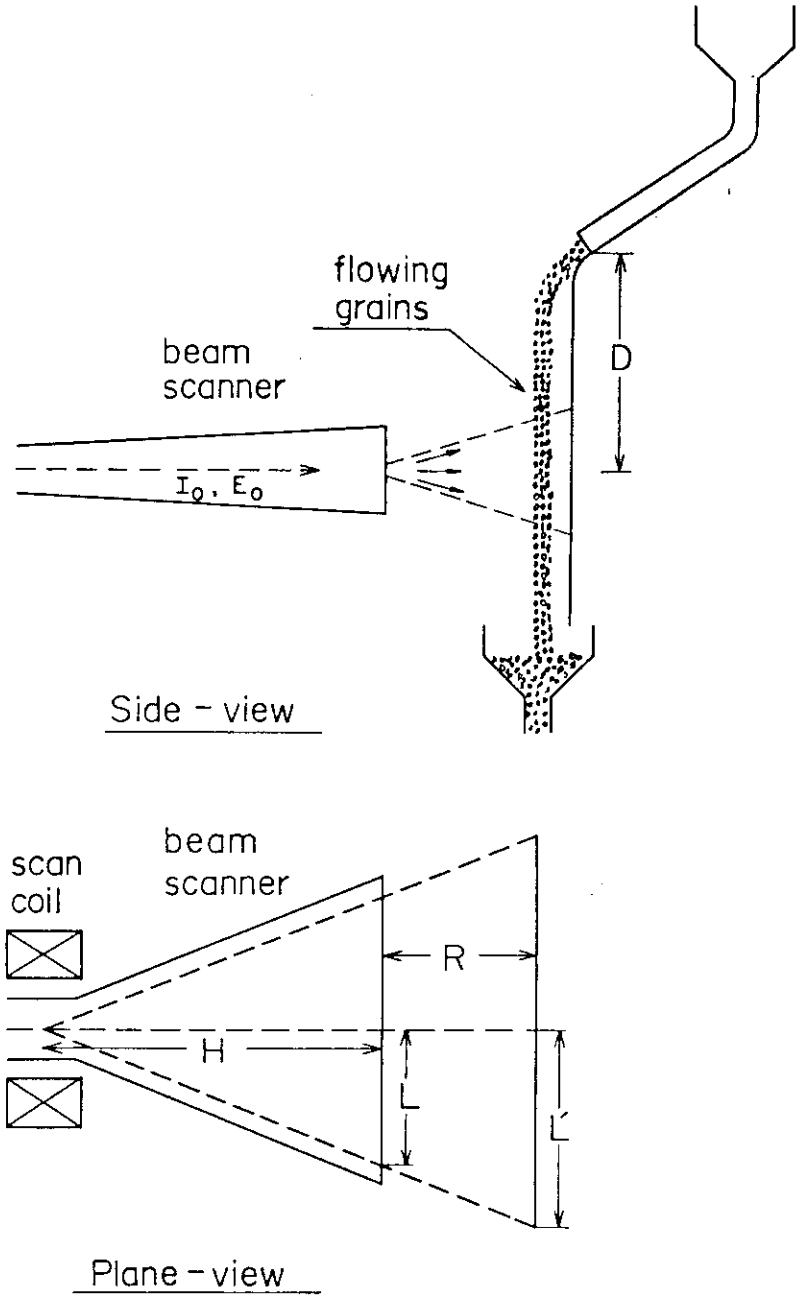

Fig. 1 A simple model of continuous-gravity-feed irradiator for disinfestation of maize with an electron accelerator

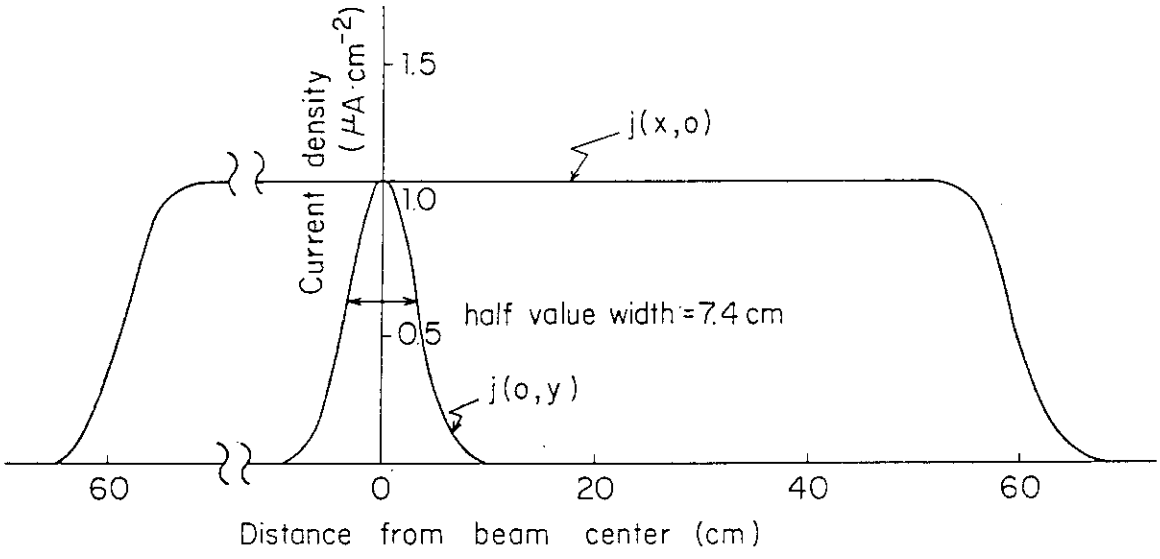

Fig. 2 Calculated average electron current density distributions in the direction of maize movement (j(o,y)) and in the direction of beam scanning (j(x,o)) for a typical irradiating condition in the Dynamitron accelerator.

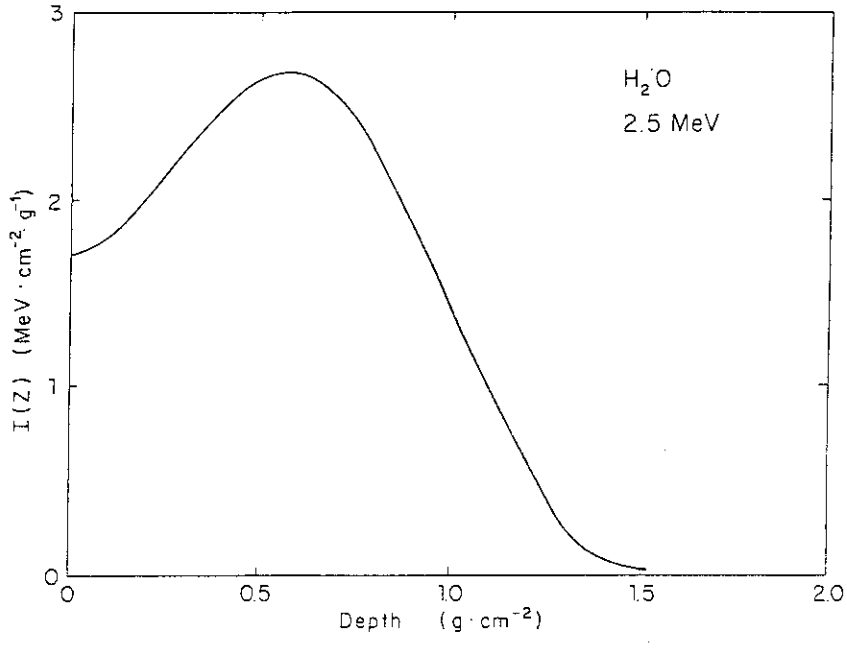

Fig. 3 The energy deposition distribution I(z) in a semi-infinite water medium for plane perpendicular beam of 2.5 MeV monoenergetic electrons given by Tabata's empirical formula[12].

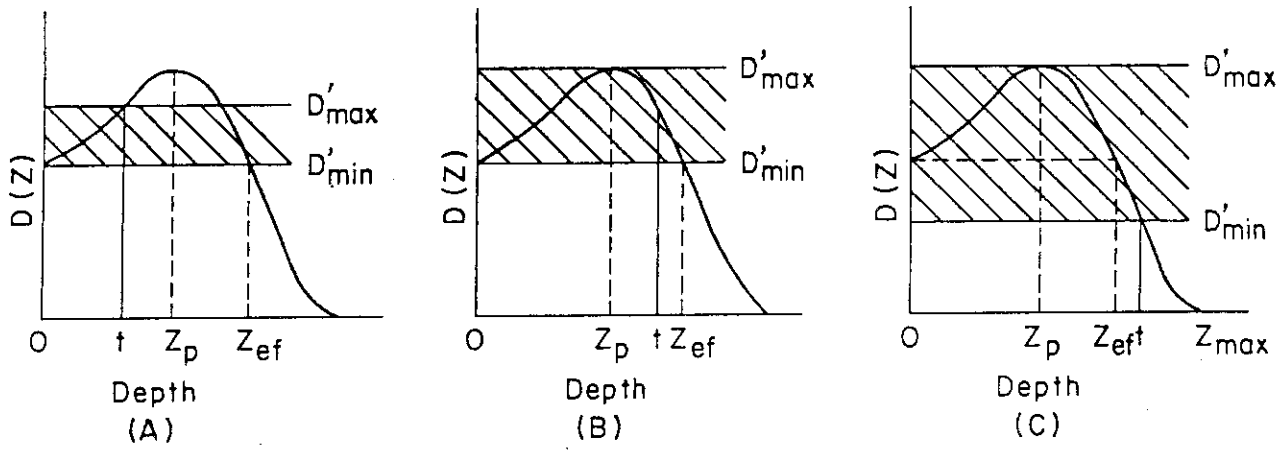

Fig. 4 Dose dispersion with increase of the absorber thickness:

(A) $0 < t \leq z_p$, (B) $z_p < t \leq z_{ef}$,

(C) $z_{ef} < t \leq z_{max}$

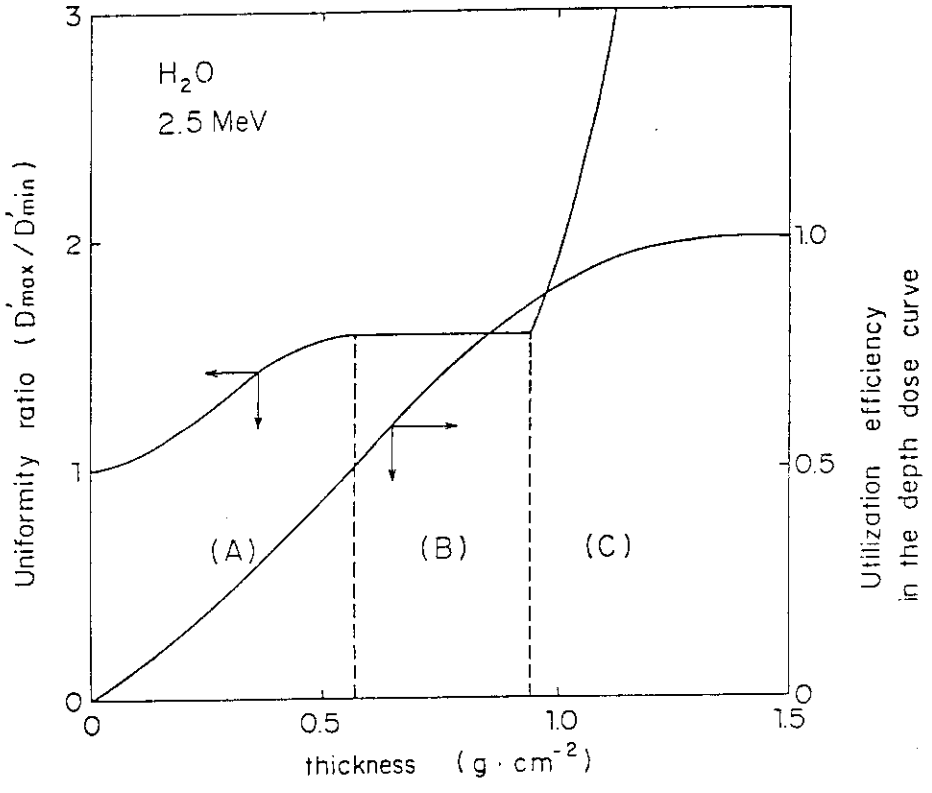

Fig. 5 The change of uniformity ratio (D'_{max}/D'_{min}) and beam utilization efficiency in the depth dose curve with absorber thickness.

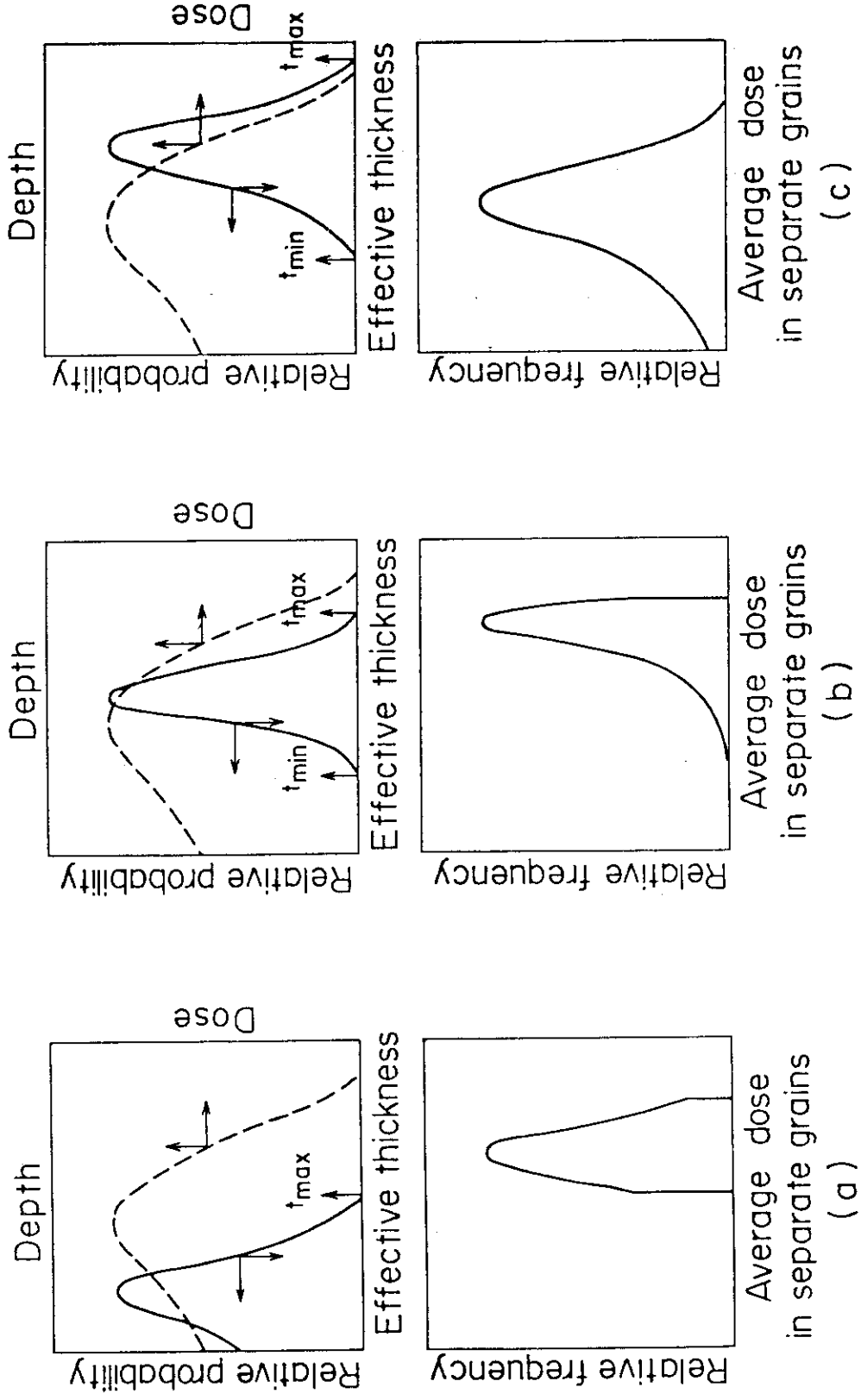

Fig. 6 Typical examples of relative frequency distribution of average doses in separate irradiated grains for given relative probability distributions in three different regions of the effective thickness.

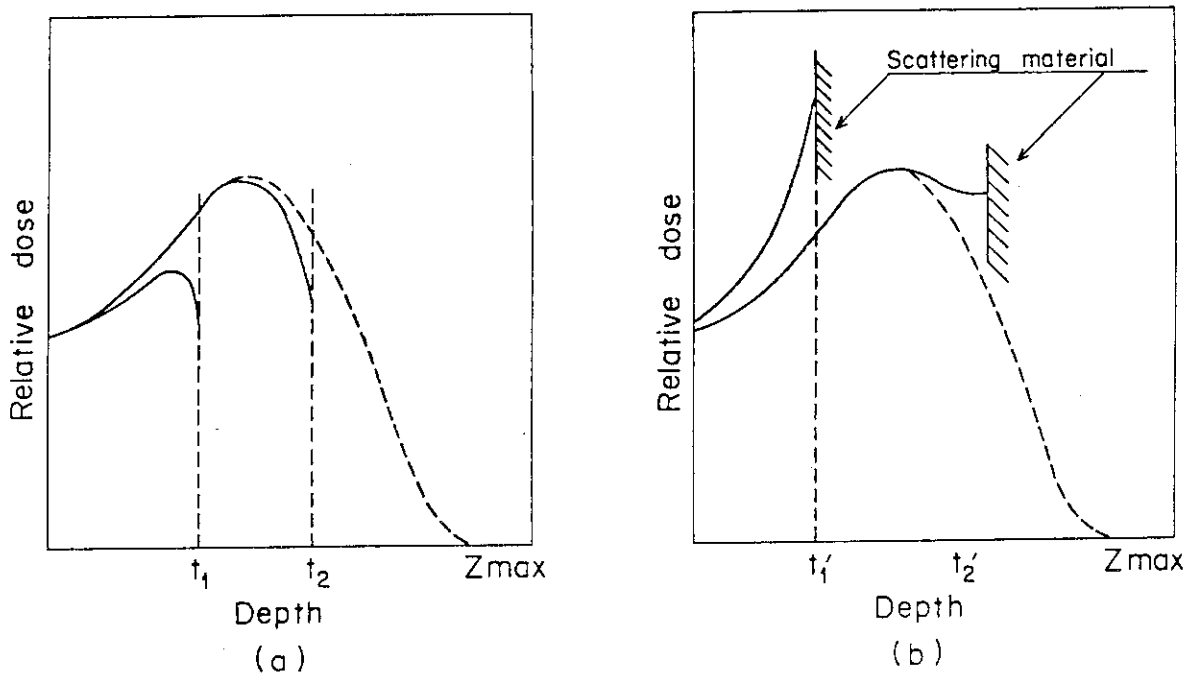

Fig. 7 Typical examples of the depth dose curves in thin absorber compared with the maximum electron range: (a) there is no scattering material behind the absorber, (b) there is some scattering material with higher effective atomic number behind the absorber.

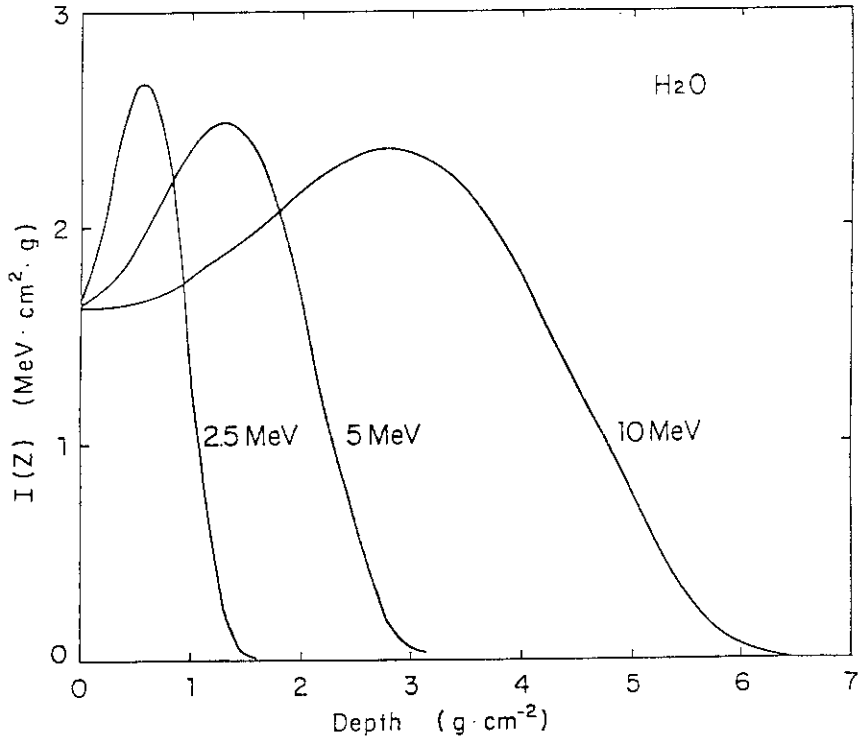

Fig. 8 The energy deposition distributions I(z) in a semi-infinite water medium for plane perpendicular beam of different monoenergetic electrons.

APPENDIX I

Calculation of Longitudinal Dose Non-Uniformity with Simultaneous Product Movement and Beam Scanning in Industrial Electron Irradiation.

1. Introduction

In many kinds of electron accelerators for industrial irradiation, dose distribution in lateral direction perpendicular to the direction of motion of the product is usually made more uniform by scanning the beam magnetically. The scan frequency and the speed of product must be co-ordinated so as to ensure that all the products is completely and uniformly irradiated with this method. Multiple overlap of successive scan traces must be always achieved for any given speed of product.

The recent increase of the beam power of these systems requires to increase the speed of product, and consequently requires to increase the scan frequency to avoid longitudinal dose non-uniformity with simultaneous product movement and beam scanning. The latter requirement is not very much important in several radiation chemical processes and radiation sterilization for medical supplies, since the required doses are more than 10 kGy. In the field of food irradiation processings such as sterilization of harmful insects in grains[1-3] and sprout inhibition in which the required doses are 1 kGy or lower, however, it is basically important to use high scan frequency to avoid the dose non-uniformity, since the flow rates of the product must be very high.

The longitudinal dose uniformity due to beam scanning depends not only on scan frequency but also other few irradiation parameters, but the quantitative relation has not been given yet between the dose non-uniformity and the irradiation parameters.

This report aims at deducing the fundamental formula generalizing the relation for steady current type electron accelerators with single beam scanning, and at obtaining the critical velocity of the product necessary for the longitudinal dose uniformity.

2. Average Electron Current Density Distribution in Radiation Field

Figure 1 shows a simplified geometrical model of electron irradiation with continuous beam and single beam scanning, where E_0 is the electron energy in the acceleration tube MeV, I_0 the beam current in the tube (A), H the height of the beam scanner (cm), 2L the scan width

on the beam window (cm), 2L is the projected scan width on the surface of the product ($L' = (H + R)L/H$), Θ the scattering angle (rad^2), R the distance from the beam window to the product surface (cm), and v the velocity of product ($cm \cdot s^{-1}$).

In this simplified model, it is assumed that (1) the distribution of the scattering angle is gaussian, (2) the effective diameter of the beam in the acceleration tube is much smaller than R, (3) scanning angle ψ_0 is small ($\cos \psi_0 \simeq 1$), (4) R is much smaller than the electron penetration range in air, (5) the intensity of the scanned beam is uniform in the lateral direction. On these assumptions, average electron current density on the product surface is expressed by the equation [4,5]:

$$j(x,y) = \frac{\eta_t I_0}{2RL'\sqrt{\pi\,\bar{\theta}_t^2}}\left(1 - \frac{\bar{\theta}_t^2}{4}\right) \exp\left\{\frac{-y^2}{R^2\bar{\theta}_t^2}\right\} \left| f(x) \pm f(-x) \right| \quad (A \cdot cm^{-2}), \tag{1}$$

where

$$f(x) = \frac{1}{2}\left[1 - \exp\left\{\frac{-4(x - L')^2}{\pi R^2 \bar{\theta}_t^2}\right\}\right]^{1/2} ,$$

where $\bar{\theta}_t^2$ is the total mean squared scattering angle (total MSSA), and η_t is the total transmission coefficient which is approximately expressed in the form $\eta_t = \eta_w \cdot \eta_a$, where η_w and η_a are the transmission coefficients for the beam window and air, respectively, given by an empirical equation[4]. The plus and the minus signs in eq. (1) are taken for $|x| \leq L'$ and $|x| \geq L'$, respectively.

In consideration of lateral displacement of electrons[7] in air due to multiple scattering in air, the total MSSA is approximately expressed in the form[4,5]

$$\bar{\theta}_t^2 = \bar{\theta}_w^2 + \frac{1}{3}\bar{\theta}_a^2 , \tag{2}$$

where $\bar{\theta}_w^2$ and $\bar{\theta}_a^2$ are MSSA in the beam window and air, respectively.

A simple theoretical expression for MSSA is given by Williams[8,6], and more accurate and complicated expression which is based on Moliére's theory is given by Hanson[9]. The experimental value of the total MSSA is approximately given from the longitudinal distribution of dose rate or electron current density on the product surface in the direction of product flow line as follows:

$$\bar{\theta}_t^2 = \frac{W_{1/2}}{4R^2} \quad , \tag{3}$$

where $W_{1/2}$ is the length in the direction of the product flow line within which dose rate or electron current density is higher than 1/e (= 0.368) value of the peak of the distribution.

3. Real Electron Current Density in Radiation Field

The electron current density according to eq. (1) means the value obtained by averaging the periodic change due to beam scanning. The real current density on the beam center axis (x = 0, y = 0) is given by the equation[4]

$$j_{0,0}(t) = \frac{\eta_t I_0}{\pi R^2 \bar{\theta}^2} \exp\left[\frac{-1}{\bar{\theta}_t^2}\left\{\frac{4L'f}{R}\left(t - \frac{N}{2f}\right)\right\}^2\right] \quad , \tag{4}$$

where t is time (s), f the scan frequency (Hz), N an arbitrary positive integer which satisfies $|t - N/2f| \leqq 1/4f$. The real current density at a point P, y cm apart from the beam center axis on the center flow line of the moving product with the velocity v $cm \cdot s^{-1}$ is approximately expressed in the form

$$j_0(t) = \frac{\eta_t I_0}{\pi R^2 \bar{\theta}_t^2} \exp\left[\frac{-1}{\bar{\theta}_t^2}\left\{\frac{4L'f}{R}\left(t - \frac{N}{2f}\right)\right\}^2\right] \exp\left\{\frac{-(vt - \alpha)^2}{R^2 \bar{\theta}_t^2}\right\}, \tag{5}$$

where α is y co-ordinate of the point P at t = 0 on the product flow line.

Figure 2 shows the change of $j_0(t)$ with time and x co-ordinate of the point v at which the beam axis of the scanned beam intersects the product surface. The function j (t) is shown in a group of separate gaussian functions formed at a regular time interval 1/2f.

4. Total Charge Fluence and Dose Non-uniformity

The total charge fluence which the point P on the product receives while passing through the radiation field is given by the integration of $j_0(t)$ over the passage time. For usual irradiating conditions in which $L' \gg R\sqrt{\bar{\theta}_t^2}$, the first exponential tirm in eq. (5) shows separate guassian distribution of the second exponential term in eq. (4). The charge fluence obtained by integration of $j_0(t)$ can be approximately expressed as follows:

$$Q_t = \int_{-\infty}^{+\infty} j_0(t)dt$$

$$= \frac{\eta_t I_0}{\pi R^2 \bar{\theta}_t^2} \left[\int_{-\infty}^{+\infty} \exp\left\{\frac{-(4L'ft)^2}{R^2\bar{\theta}_t^2}\right\} dt \cdot \left\{ \sum_{N=-\infty}^{+\infty} \exp\left\{\frac{-v^2(t_b + Nt_f)^2}{R^2\bar{\theta}_t^2}\right\} \right] \right.$$

$$= \frac{\eta_t I_0}{4R^2 L' f \sqrt{\pi\bar{\theta}_t^2}} \sum_{N=-\infty}^{+\infty} \exp\left\{\frac{-(t_b + Nt_f)^2}{t_e^2}\right\}, \qquad (6)$$

where t_b is the minimum value of the time difference from the time when the point P crosses the x-axis till the time when the scanned beam crosses the y-axis, t_f, the time interval when the beam axis of the scanned beam crosses the y-axis, and $t_e = R\sqrt{\bar{\theta}_t^2}/v$.

The equation (6) can be rewritten in the simple form

$$Q_t = Q_0 \sum_{N=-\infty}^{+\infty} \exp\left\{\frac{-(b + N)^2}{a^2}\right\} = Q_0 \cdot a \cdot f(a, b), \qquad (7)$$

where a is the velocity ratio factor ($= t_e/t_f$), b is the phase factor ($= t_b/t_f$ $0 \le b \le 1/2$), and $Q_0 = \eta_t I_0/4RL'f\sqrt{\pi\bar{\theta}_t^2}$.

Figure 3 shows the change of $a \cdot f(a, b)$ on the center flow line ($x = 0$) with the phase factor b for different values of the velocity factor a. The function f (a, b) has a constant values of $\sqrt{\pi}$ when $a \ge 1$, and it varies with the factor b when $a < 1$. Since the longitudinal distribution of Q_t on the product surface corresponds to that of absorbed dose, the result in Fig. 3 means that the longitudinal dose uniformity on the center flow line ($x = 0$) due to beam scanning is appreciable when $a < 1$.

Figure 4 shows the relative longitudinal dose distribution along the center flow line on the product surface for different values of the velocity factor a. The dose uniformity ratio which is defined by the ratio of the maximum dose to the minimum one, f (a, 0)/f (a, 0.5), for different values of a is shown in Table 1. The ratio is considered to be almost negligible for the value of a above 0.8, but the critical value necessary for complete dose uniformity equals 1.0, that is $v_e = v_f$.

5. Critical Velocity of Product

From above results, the critical velocity of the product necessary for the longitudinal dose uniformity on the center flow line (x = 0), can be expressed by the equation

$$v_{c \cdot x=0} = 2fR\sqrt{\bar{\theta}_t^2} \quad . \tag{8}$$

On non-center flow line along the product surface ($x \neq 0$), however, the intersections of the beam axis of the scanned beam and the product surface are not located in a regular interval (v/2f cm), but in a long and a short interval alternatively depending on the x co-ordinate as shown in Fig. 1. The long interval equals v/f cm on both edges of the flow line ($|x| = L'$) where the short one equals zero. Therefore the critical velocity for both edges of the flow line is given by the equation

$$v_{c,|x|=L'} = fR\sqrt{\bar{\theta}_t^2} = \frac{1}{2} v_{c,x=0} \quad . \tag{9}$$

This result means that the longitudinal dose non-uniformity due to beam scanning is most severe on both edges of the flow line.

On the whole, the effective critical velocity necessary for the longitudinal dose uniformity is decided as follows:

$$v_c = fR\sqrt{\bar{\theta}_t^2} \quad . \tag{10}$$

Equation (10) shows that the critical velocity is proportional not only to the scan frequency, but also to the distance from the beam window to the product surface and the root of the total MSSA. When the influence of the air layer on the value of $\sqrt{\bar{\theta}_t^2}$ can be neglected, the critical velocity is roughly proportional to E_0^{-1}, $Z_w^{1/2}$ and $d_w^{1/2}$ where Z_w and d_w is the atomic number and the thickness of the beam window, respectively, if the effective radius of the electron beam in the acceleration tube is much smaller than the value of R.

The value of v_c for different typical values of f, R and $\bar{\theta}_t^2$ are shown in Table 2.

When $v \leq v_c$, the equation (10) is simplified by the equation

$$Q_t = 2\sqrt{\pi} \cdot \frac{v_c}{v} \cdot Q_0$$

$$= \frac{I_0 \eta_t}{2L'v} \quad . \tag{11}$$

The value Q_t given by equation (11) is different from the integration value of equation (1), $\int j(x, y)dy$, by the factor $(1 - \overline{\theta}_t^2/4)$. This factor was given as the correction for oblique incidence to the product surface in equation (1)[5] but it is neglected in the calculation of the total charge here.

6. An Application to Radiation Processing

The relationship between absorbed dose D (Gy) and electron charge fluence Q_t ($C \cdot cm^{-2}$) for plane perpendicular and monoenergetic source is generally given by the equation

$$D(z) = 10^9 \, Q_t \, I(z) \quad , \tag{12}$$

where I(z) ($MeV \cdot cm^2 \cdot g^{-1}$) is the energy deposited per unit thickness ($g \cdot cm^{-2}$) at the depth z, assuming that one electron/cm^2 is generated at the source plane[10]. Equation (12) can be approximately applied for usual radiation fields where plane perpendicular and monoenergetic conditions are not satisfied.

When a dose requirement is given for a certain radiation processing, the following form is obtained from equations (11) and (12) for the beam current requirement:

$$I_0 = \frac{2 \times 10^{-9} L' v D(z)}{\eta_t I(z)} \tag{13}$$

Equation (13) derives the critical beam current in the acceleration tube necessary for the longitudinal dose uniformity as follows:

$$I_{0c} = \frac{2 \times 10^{-9} f L' R \sqrt{\overline{\theta}_t^2} \, D_{max}}{\eta_t I(z)_{max}} \tag{14}$$

where D_{max} is the maximum dose which is required, $I(z)_{max}$ the maximum value of I(z) ranging from 2.5 to 4 for typical organic compounds for 0.5 ~ 5 MeV electrons.

The critical value of the throughput, i.e. the amount of product to be treated with a given dose within a defined period of time, is obtained from equation (14) as follows:

$$W_t = \frac{E_0 I_{0c} f_e}{\overline{D}}$$

$$= \frac{2 \times 10^{-9} f\, f_e L' R E_0 \sqrt{\bar{\theta}_t^2}}{\eta_t I(z)_{max}} \frac{D_{max}}{\bar{D}} \quad , \tag{15}$$

where f_e is the utilization efficiency of electron energy, $\bar{D}$ the average absorbed dose in the product. Since the value of $\sqrt{\bar{\theta}_t^2}$ is roughly proportional to E^{-1}, the critical throughput does not strongly depend on electron energy.

7. Discussion

The effective radius of the beam in the acceleration tube is assumed to be much smaller than R in the equation (1). However, the influence of the beam size on the electron current distribution in radiation field is not usually neglected for small distance from the beam window. When the electron current distribution in the section of the electron beam at the beam window is assumed to be two dimensional gaussian, the equivalent total MSSA at a distance R apart from the window is approximately given by the equation[5]

$$\bar{\theta}_{te}^2 = \bar{\theta}_t^2 + \frac{\delta^2}{4R^2} \quad , \tag{16}$$

where δ cm is the effective diameter of the electron beam within which the electron current density is higher than 1/e value of the peak one. The critical velocity shown in equation (10) can be approximately corrected by using equation (16) as follows:

$$v_c = f\sqrt{R^2 \bar{\theta}_t^2 + \delta^2/4} \quad . \tag{17}$$

The influence of the effective diameter is significant for the small value of R.

The approximation in equation (6) can not applied for the extreme irradiating condition in which the assumption, $L' \gg R\sqrt{\bar{\theta}_t^2}$, is not valid. It is easily expected that the dose non-uniformity shown in Fig. 3 decreases with increase of the value of $R\sqrt{\bar{\theta}_t^2}/L'$.

In the industrial accelerators which have low electron energy below 300 keV, the angular distributions of scattered electron beam in radiation field usually show a little different shapes from gaussian one. The theoretical expressions for MSSA given by Williams[8] and Hanson[9] can not be applied for this case. A little different results from our ones results here will be obtained on the dose uniformity.

In the radiation processing to control insect infestation of grains such as corn[1,2] and rice[3] in storage, the required maximum dose is about 1 kGy or lower. Assuming that the irradiation parameters are given as follows: f = 100 Hz, L' = 50 cm, R = 10 cm, $\overline{\theta}_t^2$ = 0.05, $I(z)_{max}$ = 3.0 MeV $cm^2 \cdot g^{-1}$, η_t = 1, and the effective radius of the beam in acceleration tube is negligible, the critical beam current necessary for the longitudinal dose uniformity is 7.5 mA. This value is much lower than the typical ratings of recent powerful industrial accelerators. The results here show that it is necessary to use higher scan frequency than usual values (100 ~ 300 Hz) when the require maximum dose is smaller than a few kGy.

8. Summary

For steady current type electron accelerators with single beam scanning, a fundamental formula is obtained for the relation between the longitudinal dose non-uniformity with simultaneous product movement and beam scanning and several irradiation parameters. Based on the relation, the critical velocity of the product necessary for the dose uniformity is given by the product of scan frequency, the distance from beam window to product surface, and the root of the total mean squared scattering angle.

The results are expected to be useful for various irradiator designs for electron radiation processing and the calculation method will be applied for calculation of lateral dose non-uniformity in pulse beam accelerators.

References

(1) Adem, E., Uribe, R.M., Watters, F.L., and Bourges, H., Radiat. Phys. Chem. 18, 555 (1981).

(2) Adem, E., Uribe, R.M., and Watters, F.L., Radiat. Phys. Chem. 14, 663 (1979).

(3) IAEA-TECDOC-258, International Atomic Energy Agency, Vienna (1981).

(4) Tanaka, R., Sunaga, H., Yotsumoto, K., Mizuhashi, K., and Tamura, N., Radiat. Phys. Chem. 18, 927 (1981).

(5) Tanaka, R., Oyo Butsuri 48, 432 (1979) (in Japanese).

(6) Tabata, T., and Ito, R., Nucl. Inst. and Meth. 127, 429 (1975).

(7) Rossi, B.B., and Greisen, K.I., Rev. Mod. Phys. 13, 240 (1941).

(8) Williams, E.J., Proc. R. Soc. London A169, 531 (1939).

(9) Hansen, A.O., et al., Phys. Rev. 84, 634 (1951).

(10) Spencer, L.V., NBS Monograph 1, National Bureau of Standards (1959).

TABLE A-1 Dose uniformity Ratio as a function of the velocity ratio factor a.

a	$\frac{f(a,0)}{f(a,0.5)}$
1.0	1.000
0.9	1.001
0.8	1.008
0.7	1.032
0.6	1.122
0.5	1.408
0.4	2.394
0.3	8.065

TABLE A-2 The value of the critical velocity for different typical values of f, R and $\bar{\theta}_t^2$ on the assumption that the effective beam diameter in the aceleration tube is much smaller than R.

f (Hz)	R (cm)	$\bar{\theta}_t^2$ (radian^2)	V_c (cm. s^{-1})
100	5	0.02	71
100	10	0.05	224
100	10	0.1	316
200	10	0.1	632
200	10	0.2	894

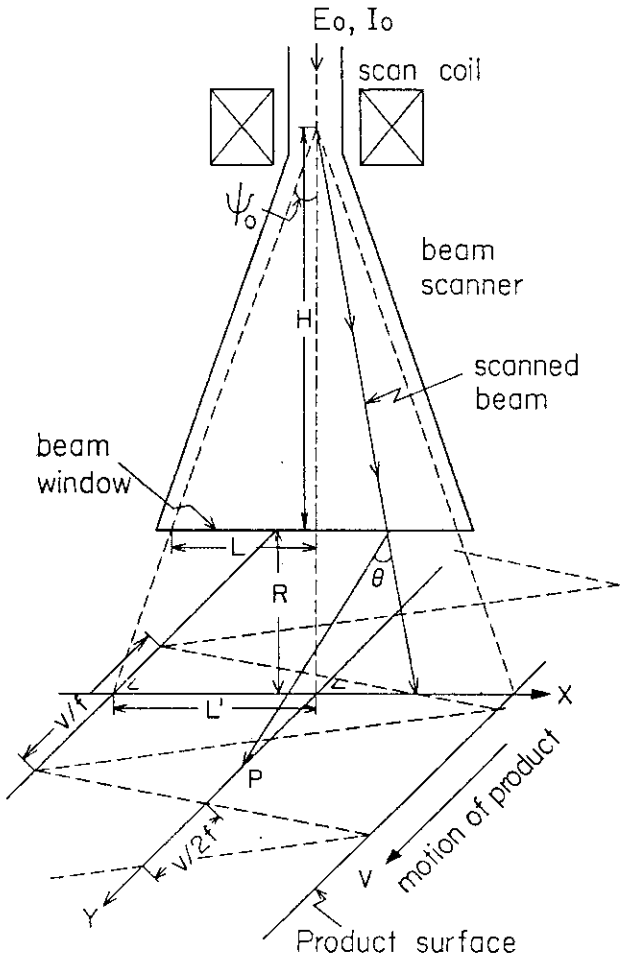

Fig. A-1 A simplified geometric model of electron irradiatio- with continuous beam and single beam scanning.

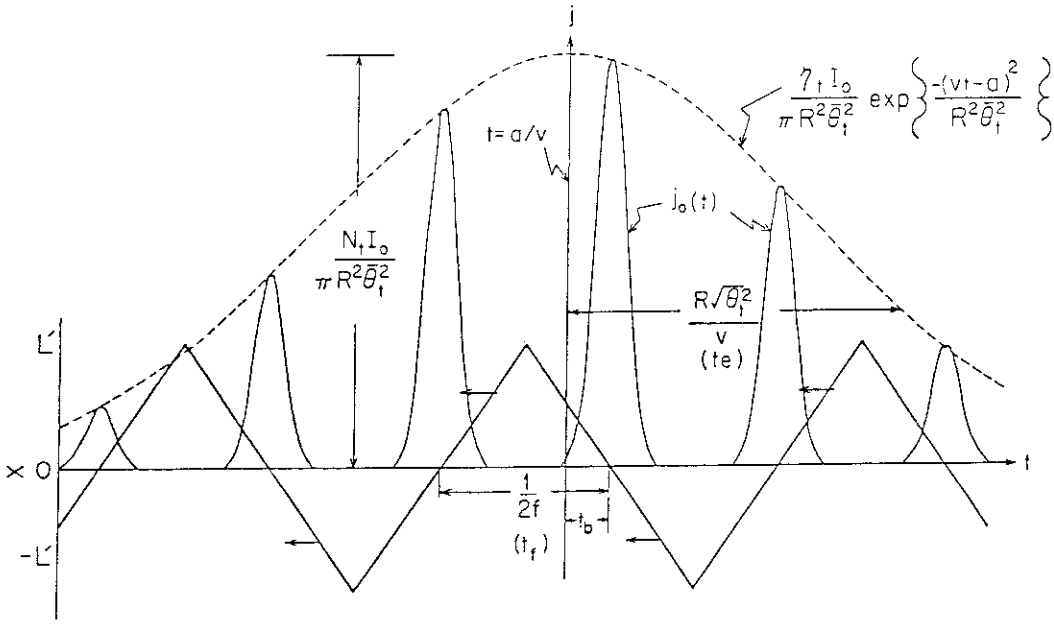

Fig. A-2 The change of $j_0(t)$ with time and x co-ordinate of the point at which the beam axis of the scanned beam intersects the product surface.

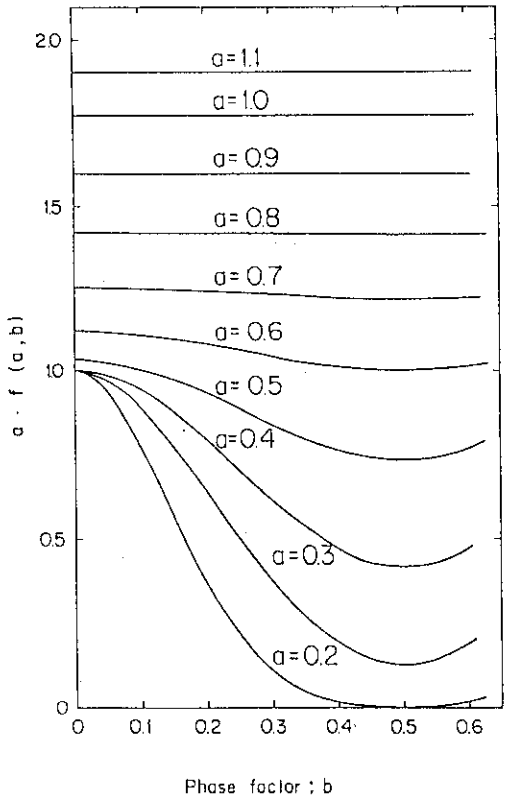

Fig. A-3 The change of a·f(a, b) on the center flow line of the product (x = 0) with the phase factor b for different values of the velocity factor a.

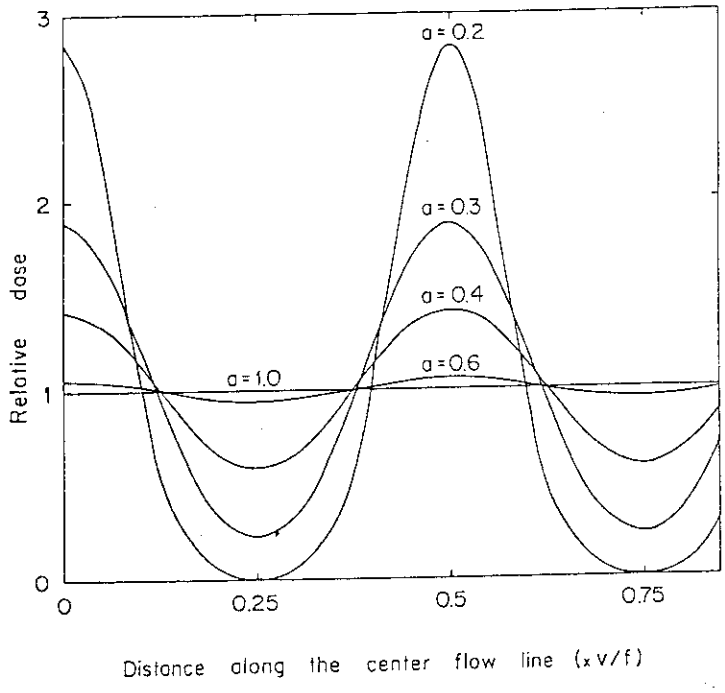

Fig. A-4 The relative longitudinal dose distribution along the center flow line on the product surface for different values of the velocity factor a.

APPENDIX II

Reference Data on Transmission, Scattering and Absorption of 2.5 and 3 MeV Electrons in Thick Layer of Matter.

Some basic data on transmission, scattering and absorption of 2.5 MeV electrons in thick layer of matter are useful for basic studies of radiation effect and irradiation technique on radio-disinfestation of maize. The data here were calculated using ETRAN code[1] and some empirical equations. The data on backscattering from thick tungsten were calculated by ETRAN code for 3 MeV electrons. Plane perpendicular beam condition is assumed for all the calculations.

REFERENCES

(1) Berger, M.J., and Seltzer, S.M., "RSIC Computer Code Collection, ETRAN Monte Carlo Code System for Electron and Photon Transport through Extended Media", CCC-107 Oak Ridge National Laboratory (1969).
(2) Tabata, T., and Ito, R., Nucl. Inst. and Meth. 127, 429 (1975).
(3) Tabata, T., and Ito, R., Nucl. Instr. and Meth. 94, 509 (1971).
(4) Hanson, A.O., et al., Phys. Rev. 84, 634 (1951).
(5) Tabata, T., and Ito, R., Nucl. Sci. Engng. 53, 226 (1974).

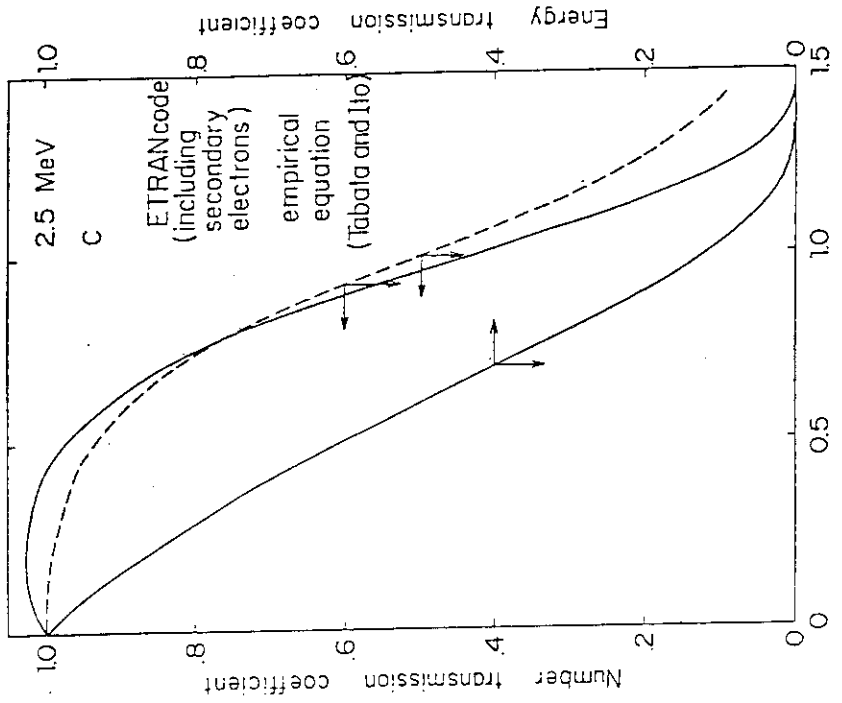

Fig. A-6 Number and energy transmission coefficients of 2.5 MeV electrons in thick layer of carbon. In the empirical equation[2] to calculate number transmission coefficient, the number of electtons is close to the number of transmitted primary electrons.

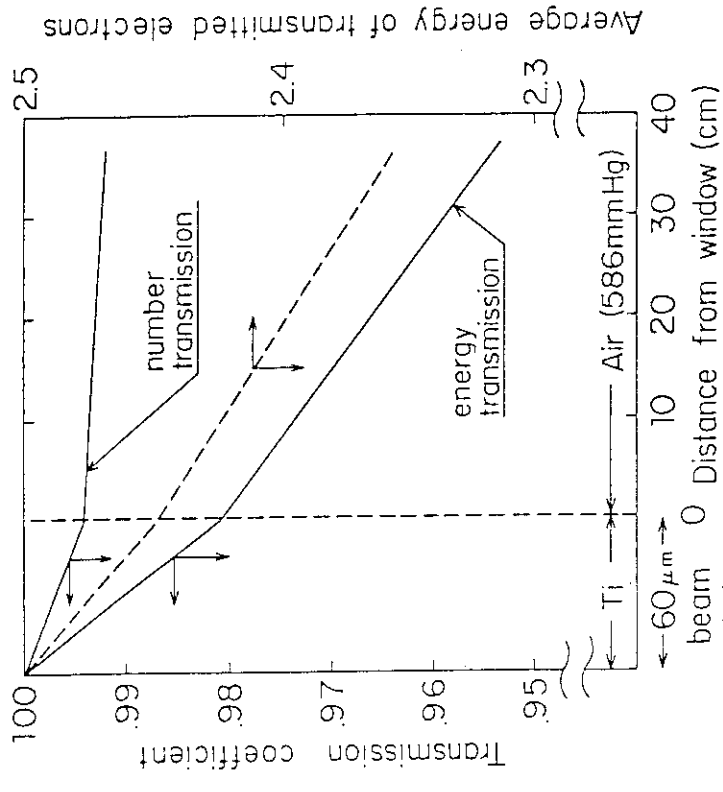

Fig. A-5 Number and energy transmission coefficients and average energy of transmitted electrons in a titamium beam window of the Dynamitron accelerator (60 μm thick) and air layer in the radiation field for 2.5 MeV electrons in the acceleration tube.

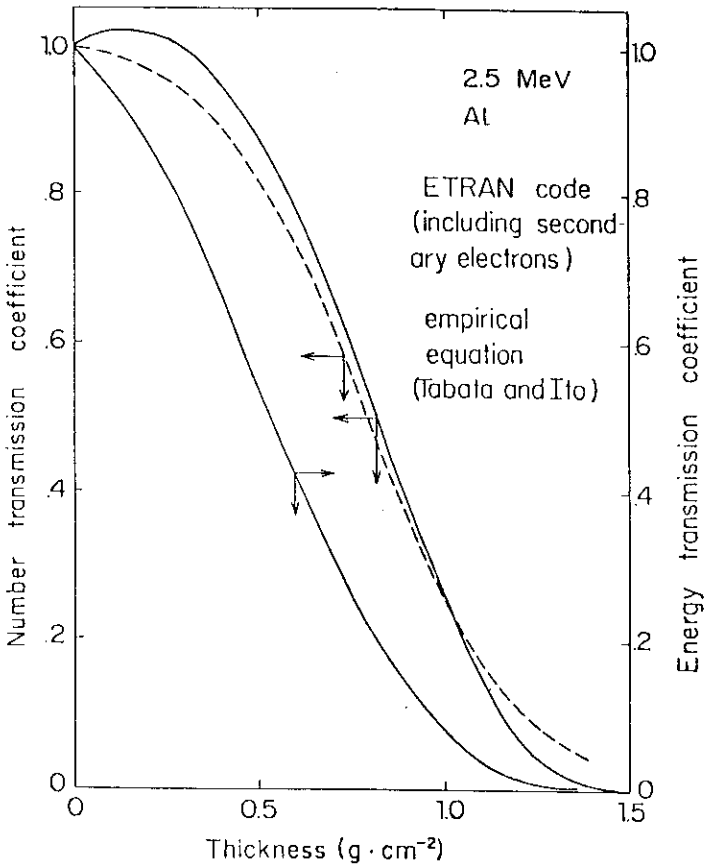

Fig. A-7 Number and energy transmission coefficients of 2.5 MeV electrons in thick layer of Aluminium. In the empirical equation[2] to calculate number transmission coefficient, the number of electrons is close to the number of transmitted primary electrons.

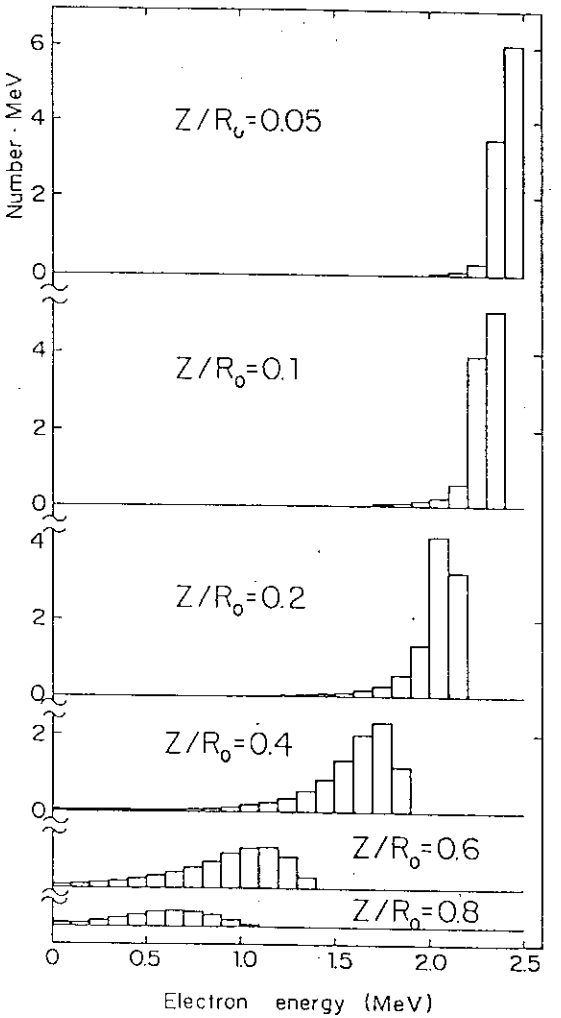

Fig. A-8 Electron energy spectra at different depths, z, of Carbon for incident electrons of 2.5 MeV (R_0: continuous slowing down approximation range, R_0 = 1.404 g·cm^{-2} for carbon at 2.5 MeV).

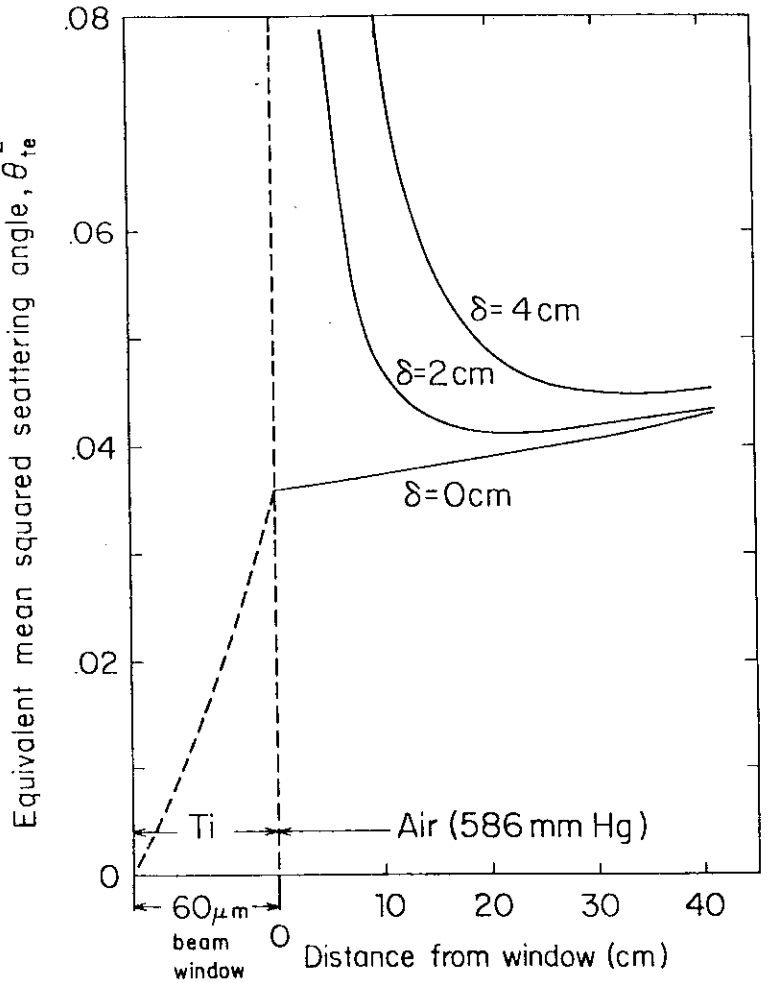

Fig. A-9 Equivalent mean squared scattering angle of transmitted electrons as a function of distance from beam window in air for different effective diameters of the electron beam in the acceleration tube (see Appendix I). The mean squared scattering angle was calculated by Hanson's approximation formula[4].

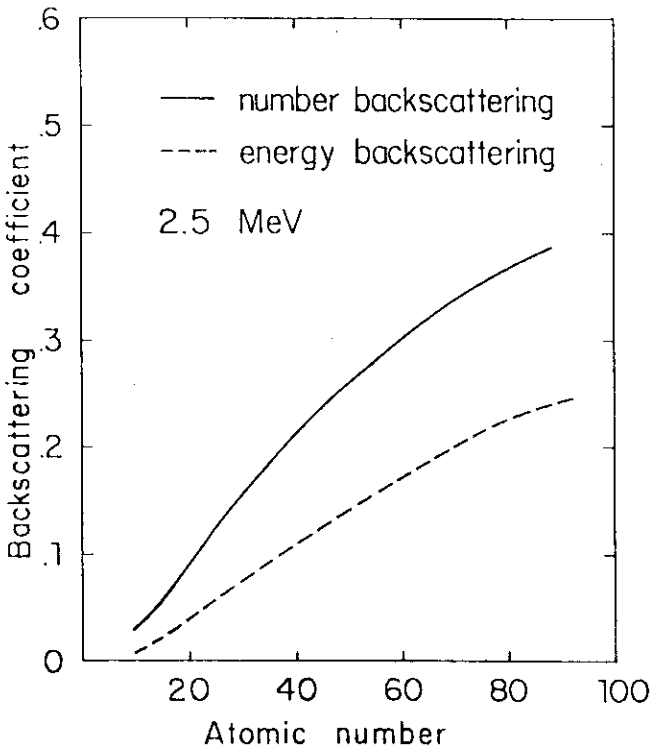

Fig. A-10 Number and energy backscattering coefficient of incident electrons of 2.5 MeV for matters as functions of atomic number.

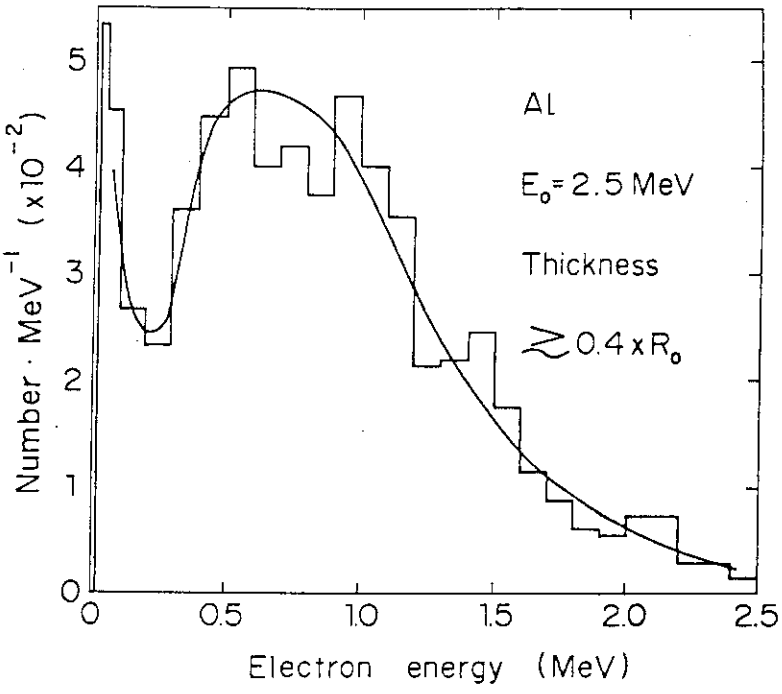

Fig. A-11 Energy spectrum of backscattered electrons from thick Aluminium Layer for incident electrons of 2.5 MeV (ETRAN code).

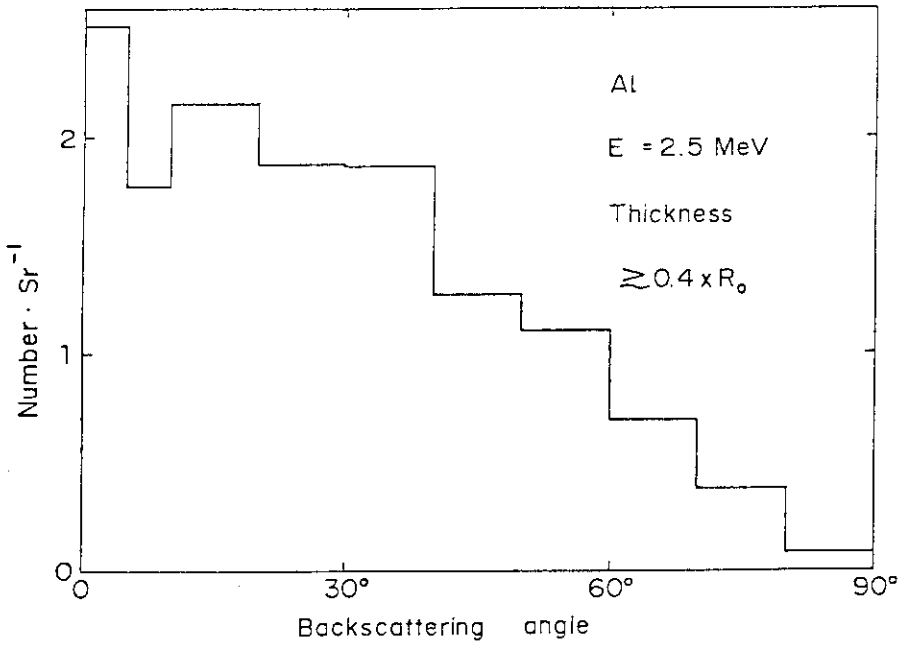

Fig. A-12 Angular distribution of backscattered electrons from thick aluminium layer for incident electrons of 2.5 MeV (ETRAN code).

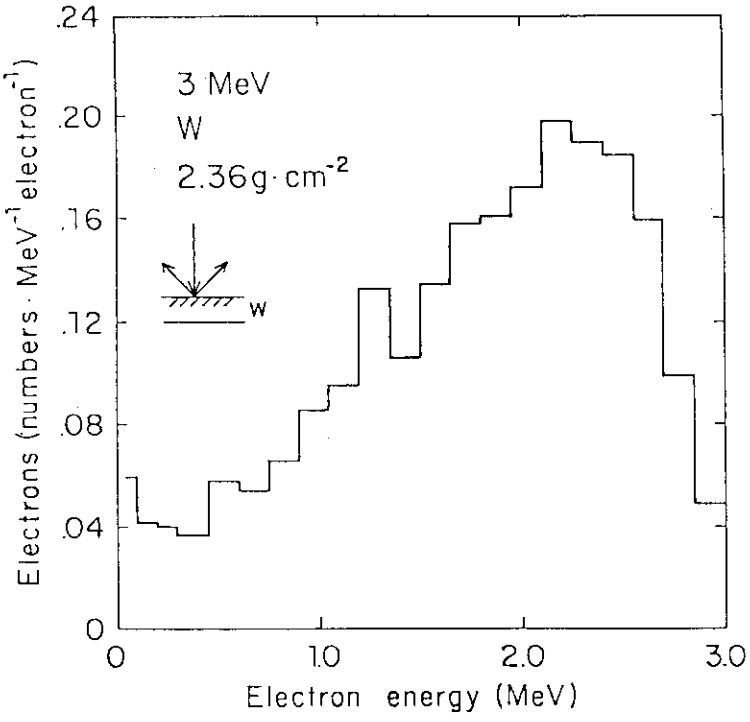

Fig. A-13 Energy spectrum of backscattered electrons from thick tungsten layer from incident electrons of 3 MeV (ETRAN code).

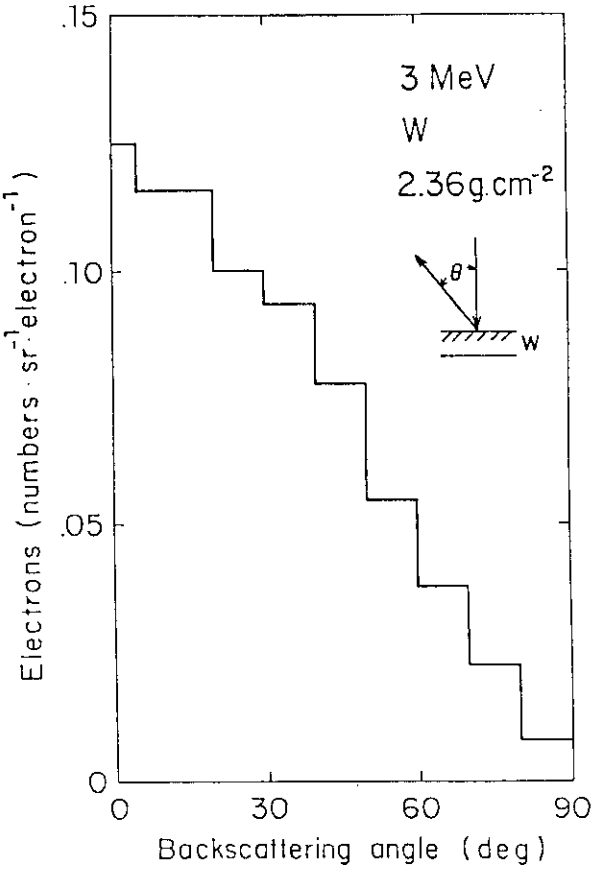

Fig. A-14 Angular distribution of backscattered electrons from thick tungsten layer from incident electrons of 3 MeV (ETRAN code).

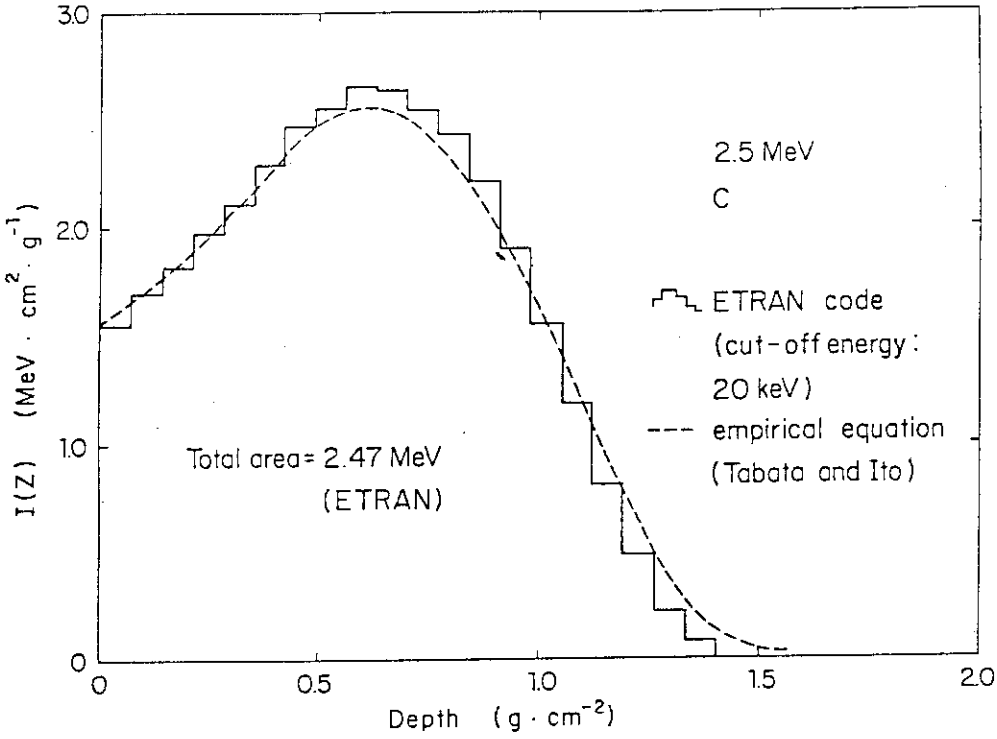

Fig. A-15 Energy deposition distribution of 2.5 MeV electrons in the semi-infinite absorber of carbon obtained with ETRAN code and an empirical equation[5].

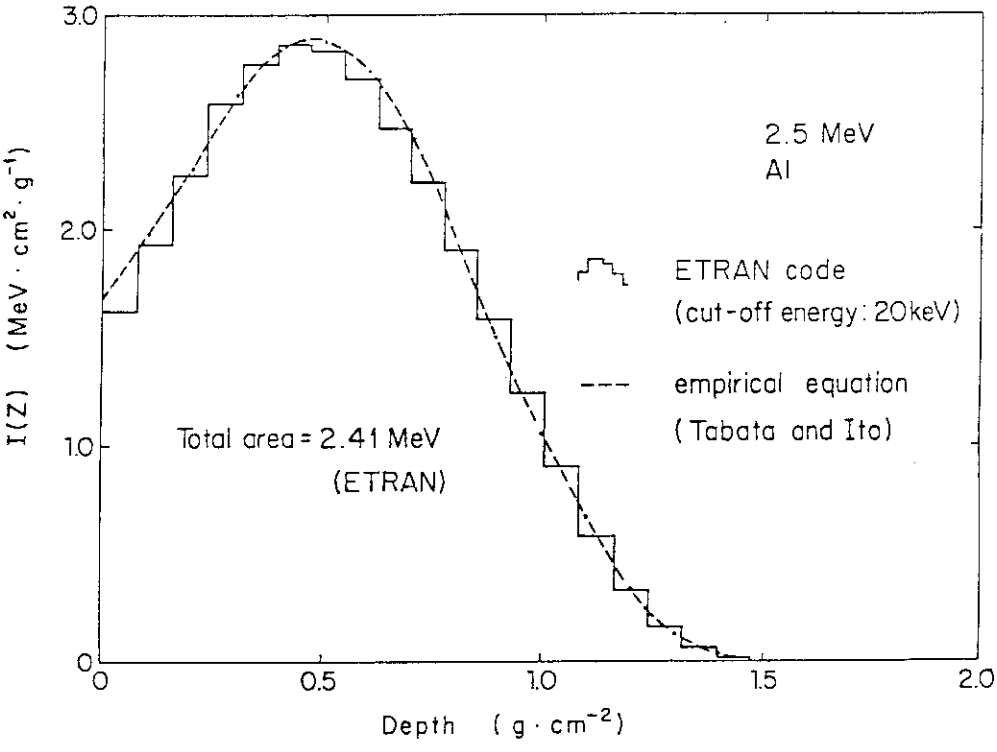

Fig. A-16 Energy deposition distribution of 2.5 MeV electrons in the semi-infinite absorber of Aluminium obtained with ETRAN code and an empirical equation[5].

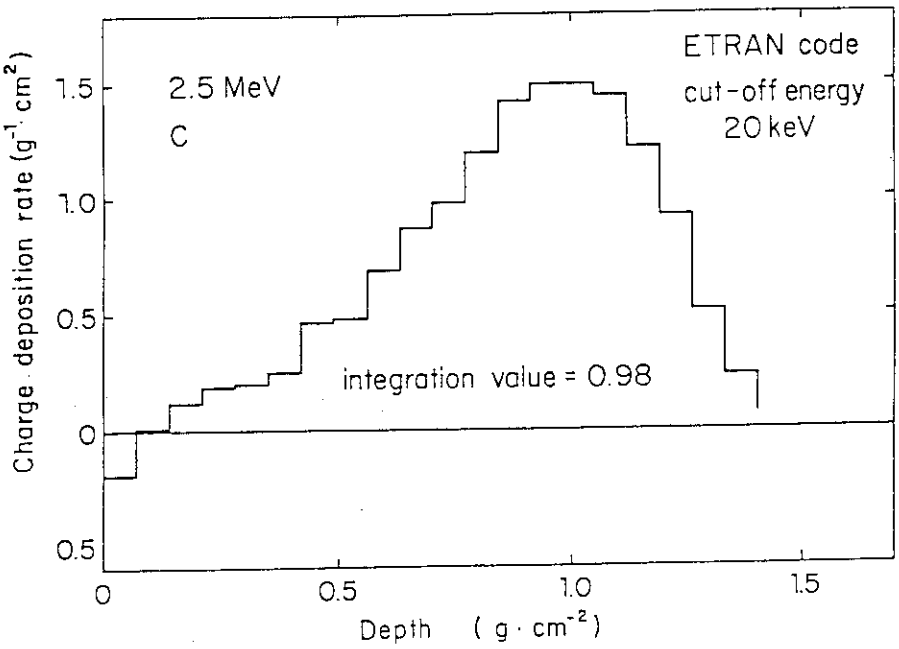

Fig. A-17 Charge deposition distribution of 2.5 MeV electrons in the semi-infinite absorber of carbon obtained with ETRAN code.

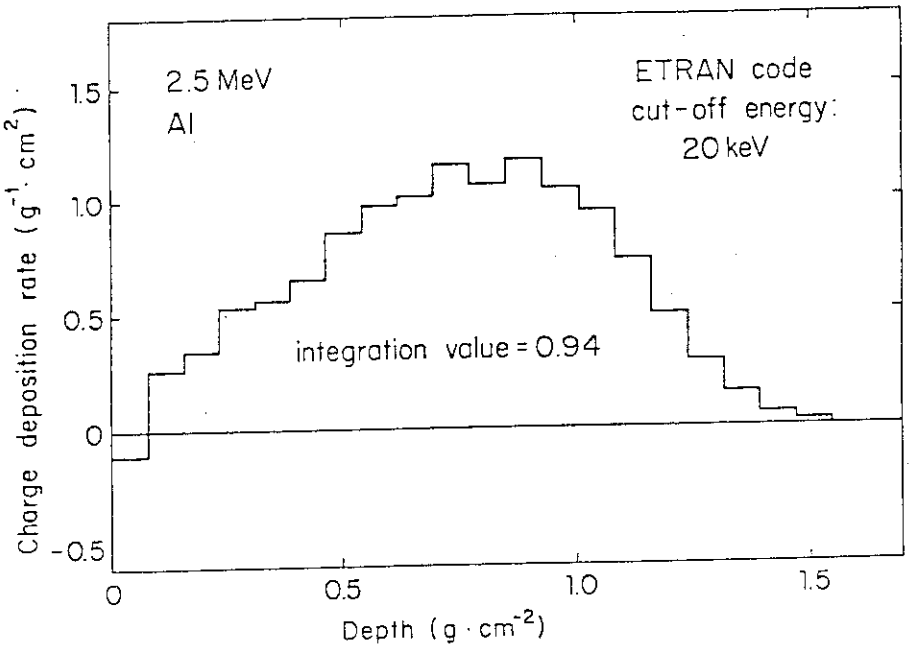

Fig. A-18 Charge deposition distribution of 2.5 MeV electrons in the semi-infinite absorber of carbon obtained with ETRAN code.